



# Dry Reforming of CO<sub>2</sub> from Industrial Off-gases in an Internal Combustion Engine: A Modelling Study

Vertieferarbeit

Daniel Schmider

Karlsruhe Institute of Technology  
Institute for Chemical Technology and Polymer Chemistry

Reviewer: Prof. Dr. Olaf Deutschmann

Advisor: Hendrik Gossler

Duration: January 7, 2019 – May 6, 2019





### Erklärung

Ich versichere wahrheitsgemäß, die vorliegende Arbeit selbstständig verfasst, alle benutzten Hilfsmittel vollständig und genau angegeben und alles kenntlich gemacht zu haben, was aus Arbeiten Anderer unverändert oder mit Abänderungen entnommen wurde; sowie die Satzung des KIT zur Sicherung guter wissenschaftlicher Praxis in der jeweils gültigen Fassung beachtet zu haben.

Karlsruhe, den 6. Mai 2019

## Acknowledgements

First and foremost, I would like to thank Prof. Deutschmann for providing me with the opportunity of completing this thesis in his working group and for selecting this interesting topic.

I would also like to thank Hendrik Gossler for providing me with instructions, guidance, and any additional help needed, as well as the CaRMeN software, which reduced the workload necessary for this study significantly and only made aspects of it possible at all.

I am grateful to my friends who helped proofread this thesis.

This thesis was written in context of the DFG research project FOR1993. The financial support for this project is gratefully acknowledged. Finally, I acknowledge the Steinbeis-Transferzentrum 240 Reaktive Strömung for making a license to the DETCHEM library available free of cost.

## Zusammenfassung

Die Reformierung von  $\text{CO}_2$  aus industriellen Abgasen ist eine vielversprechende neue Anwendungsmöglichkeit von Verbrennungsmotoren. Der Vorgang, als Polygenerationsprozess charakterisiert, ist dafür konzipiert, Synthesegas ( $\text{CO}$  und  $\text{H}_2$ ), mechanische Arbeit, und Wärme zu produzieren. Die Umwandlung der industriellen Abgase, die maßgeblich zu den weltweiten Treibhausgasemissionen und damit dem Treibhauseffekt beitragen, könnte ein wichtiger Schritt zur Verlangsamung des Klimawandels sein und stellt die primäre Motivation für diese Arbeit dar.

Um die Eignung dieses Ansatzes zu überprüfen, wurde eine Modellierungsstudie durchgeführt. Das verwendete Modell,  $\text{DETCHEM}^{\text{ENGINE}}$ , simuliert den Verbrennungsmotor als Batch-Reaktor mit variablem Volumenprofil, beinhaltet ein Wärmeübertragungsmodell und wird mit detaillierten Gasphasenreaktionsmechanismen ausgestattet. Dieses Modell wurde verwendet, um den Effekt verschiedener Parameter, wie Motorabmessungen, Drehzahl und dem Anfangszustand des Einlassgases, auf den Prozess zu analysieren. Dabei wurde der Umsatz von Kohlenstoffdioxid als die zu maximierende Größe betrachtet. Es wurde gezeigt, dass die Einlasstemperatur, das Verdichtungsverhältnis, und die Drehzahl des Motors den größten Einfluss auf den Umsatz haben. Zusätzlich wurden die Auswirkungen der Zusammensetzung des eingelassenen Gases untersucht. Verschiedene Mischungen wurden untersucht und eine Optimierung bezüglich den Verhältnissen der verwendeten Abgase und Luft durchgeführt. Die Effekte verschiedener Additive auf die minimale, zur Zündung benötigte, Einlasstemperatur wurden ebenfalls überprüft und es stellte sich heraus, dass Argon und Ozon diese Temperatur signifikant verringern können. Weiterhin wurde die Reformierung von  $\text{CO}_2$  in Deponiegas in Bezug auf die Zusammensetzung der Motorladung untersucht.

## Abstract

The dry reforming of carbon dioxide contained in industrial off-gases is a promising new application of an internal combustion engine. Categorized as a polygeneration process, it is designed to output syngas (CO and H<sub>2</sub>), work and heat. The conversion of steelworks off-gases, which contribute greatly to global greenhouse gases emissions and therefore the greenhouse effect, could be an important step towards slowing down climate change and was the primary motivation behind this work.

To investigate the validity of this approach, a modeling study focused on this process has been conducted. The utilized model, DETCHEM<sup>ENGINE</sup>, simulates the engine as a homogeneous batch reactor with a variable volume profile. It includes a heat transfer model and is equipped with detailed gas-phase reaction mechanisms. This model has been used to study the effect of a range of parameters, including geometric properties of the engine and operating conditions, on the process, with the conversion of carbon dioxide as the main focus. It has been shown that initial temperature, engine speed and the engine compression ratio have the greatest effect on carbon dioxide conversion. Additionally, the effect of the gas composition has been evaluated. Different mixtures have been evaluated and an optimization concerning the proportions of the different off-gases and air has been performed. The effects of various additives on the minimum intake temperature necessary for ignition have also been investigated, predicting that ozone and argon both lower the ignition temperature significantly. Furthermore, the conversion of CO<sub>2</sub> contained in landfill gas has been analyzed with respect to the composition of the intake gas.



# Contents

List of Acronyms	ix
List of Symbols	x
1 Introduction	1
2 Simulation details	5
2.1 Reactor model . . . . .	5
2.1.1 Modeled systems . . . . .	8
2.2 Chemical model . . . . .	9
2.3 Process workflow and automation . . . . .	9
3 Results	13
3.1 General reaction observations . . . . .	13
3.2 Effects of engine parameters on CO <sub>2</sub> conversion . . . . .	15
3.2.1 Connecting rod length . . . . .	16
3.2.2 Bore and stroke . . . . .	16
3.2.3 Compression ratio . . . . .	18
3.2.4 Engine speed . . . . .	19
3.2.5 Wall temperature . . . . .	24
3.3 Effects of inlet conditions . . . . .	26
3.3.1 Initial temperature . . . . .	26
3.3.2 Initial pressure . . . . .	29
3.4 Effect of the employed reaction mechanism . . . . .	30
3.5 Effect of the gas composition . . . . .	32
3.5.1 Primary gas proportions . . . . .	32
3.5.2 Optimization of the gas composition . . . . .	34
3.5.3 CO <sub>2</sub> conversion without prior methane combustion . . . . .	36
3.5.4 Effect of additives on ignition temperature and conversion . . . . .	39
3.6 Landfill gas conversion in an internal combustion engine . . . . .	44
4 Conclusion and outlook	47



# List of Acronyms

BDC	Bottom dead center
BFG	Blast furnace gas
BOFG	Basic oxygen furnace gas
CaRMeN	Catalytic Reaction Mechanism Network
CI	Compression ignition
COG	Coke oven gas
DETCHEM	Detailed Chemistry
DME	Dimethyl ether
GHG	Greenhouse gas
HCCI	Homogeneous charge compression ignition
ICE	Internal combustion engine
LFG	Landfill gas
RCM	Rapid compression machine
rpm	Revolutions per minute
SI	Spark ignition
TDC	Top dead center

# List of Symbols

$a$	Crank radius (m)
$A$	Area (m <sup>2</sup> )
$\alpha$	Woschni scaling factor
$B$	Bore (m)
$C_1$ and $C_2$	Empirical constants according to Woschni (2.892 and 3.24 · 10 <sup>-3</sup> m/s/K, respectively)
$\bar{c}_{\text{piston}}$	Piston velocity (m s <sup>-1</sup> )
$c_s$	Concentration of species $s$ (mol m <sup>-3</sup> )
$\bar{c}_V$	Mean heat capacity at constant volume (J mol <sup>-1</sup> K)
$F$	Ratio of connecting rod length and crank radius
$h$	Heat transfer coefficient according to Woschni (W m <sup>-2</sup> K <sup>-1</sup> )
$H$	Molar enthalpy (J/mol)
$\Delta H^0$	Molar reaction enthalpy at standard conditions (J mol <sup>-1</sup> )
$k_j$	Rate constant of reaction $j$ (mol, s, m <sup>3</sup> dependent on reaction order)
$l$	Connecting rod length (m)
$L$	Stroke (m)
$N$	Engine speed (s <sup>-1</sup> )
$N_R$	Number of reactions
$N_S$	Number of species
$\nu$	Stoichiometric coefficient
$\dot{\omega}$	Rate of formation (mol m <sup>-3</sup> s <sup>-1</sup> )
$p$	Pressure (bar)
$\pi$	Geometric constant (3.1415)
$\dot{q}$	Heat flux (J s <sup>-1</sup> )
$R$	Ideal gas constant (8.314 J mol <sup>-1</sup> K <sup>-1</sup> )
$r_c$	Compression ratio
$\sigma$	Stroke ratio
$T$	Temperature (K)
$\Theta$	Crank angle (°)
$V$	Volume (m <sup>3</sup> )
$\dot{V}$	Volume change (m <sup>3</sup> s <sup>-1</sup> )

$V_c$	Clearance volume ( $\text{m}^3$ )
$V_d$	Displaced volume ( $\text{m}^3$ )
$w$	Gas velocity ( $\text{m s}^{-1}$ )
$X$	Conversion (%)
$Y$	Absolute amount converted (%)
$Z_i$	Percentage of primary gas $i$ in gas mixture (%)



# 1 Introduction

## 1.1 Environmental background

The emission of greenhouse gases (GHG) is an increasingly relevant problem for today's and tomorrow's society. Carbon dioxide is the most prevalent greenhouse gas from anthropogenic sources [1] and is the largest contributor to the man-made greenhouse effect [2]. The largest CO<sub>2</sub>-producing sectors worldwide are electricity and thermal energy (25%), agri- and horticulture (24%), the goods industry (21%) and transport (14%) [1]. To curb the progression of climate change, finding new ways of limiting greenhouse gas emissions is crucial. The use of fossil fuels is a major component of that progress, limiting their use and therefore emissions is imperative to slow down their accumulation in the atmosphere. From an economic perspective, emission control is promoted via the trade of carbon dioxide certificates, which provides a financial incentive to reduce, capture or convert any accumulating CO<sub>2</sub>.

## 1.2 The role of the steel industry in greenhouse gas emissions

Greenhouse gas emission statistics show that the iron and steel industry is responsible for 6% to 7% of total anthropogenic carbon dioxide emissions, corresponding to about a third of the whole industry sector [3]. This is only considering the emissions stemming from the directly involved processes, i.e. the necessary electricity and its sources are not included. Like many metallurgical upgrading processes, steel production utilizes coke to reduce oxidic ores to the respective metal. Other major metals whose refining process utilize coke include aluminum, copper, nickel and zinc, but they possess only a minor share of the beneficiation sector compared to steel [4]. The use of coke as a reducing agent is the main culprit of CO<sub>2</sub> generation inside metallurgic plants. 73.4% of world steel production is based on the integrated steelmaking method, which generates three main off-gases: coke oven gas (COG), originating from the coke-making process, blast furnace gas (BFG) and basic oxygen furnace gas (BOFG) [5]. The compositions of these three gases are listed in Table 1.1.

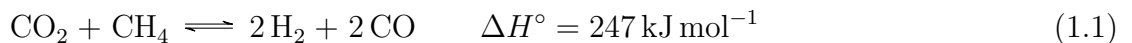
**Table 1.1:** Compositions (in %) of the three main steelwork off-gases and their volumetric flow rate for a modern steel plant with a production of 6 Mt/a

	COG	BFG	BOFG
CO <sub>2</sub>	1.2	21.6	20.0
CO	4.1	23.5	54.0
H <sub>2</sub>	60.7	3.7	3.2
CH <sub>4</sub>	22.0	0.0	0.0
KW	2.0	0.0	0.0
N <sub>2</sub>	5.8	46.6	43.8
H <sub>2</sub> O	4.0	4.0	4.0
Ar + O <sub>2</sub>	0.2	0.6	0.7
volumetric flow rate / Nm <sup>3</sup> h <sup>-1</sup>	40000	730000	35000

While other industrial routes such as the smelting reduction process can potentially lower CO<sub>2</sub> emissions [6], CO<sub>2</sub> conversion or storage methods for the gases produced in the widely-used integrated process are also worth investigating.

### 1.3 Dry reforming inside internal combustion engines

An example for a reaction converting CO<sub>2</sub> is dry reforming (Eq. 1.1), which uses methane as a reducing agent in order to produce syngas:



The reaction is strongly endothermic and therefore requires high temperatures to proceed in the desired direction, resulting in high operation expenses. Catalytic approaches have been shown to present problems such as catalyst oxidation or coking [7, 8]. On the other hand, the possibility of conducting this reaction in an internal combustion engine seems promising and presents multiple advantages. First and foremost, the compression during an engine cycle provides high temperatures to overcome the thermodynamic and kinetic hindrances of the dry reforming reaction. Additionally, engines are very flexible in their operation and are able to react to changing conditions quickly. Furthermore, engines are well-suited to make use of the work generated during operation, which improves the overall process efficiency. Utilizing an internal combustion engine as a reactor to simultaneously produce valuable chemicals and output work characterizes it as a polygeneration device. The concept of polygeneration describes the operation of a reactor or a machine with more than one type of energy output, for example heat, electricity, work or chemical energy. The flexibility of these systems can enable the immediate use of one type of energy while another is stored away during energy surplus periods as a precaution for energy shortages, both of which are common in power grids consisting mainly of renewable energy sources.

The aptitude of internal combustion engines for the purpose of dry reforming has been investigated by Gossler et al., who found positive results, indicating that up to 50 % of CO<sub>2</sub> in the inlet gas could be converted using relatively mild initial conditions [9]. In their work, the temperatures necessary for the dry reforming reaction to proceed were achieved by initially burning a portion of the fuel. While the combustion of methane produces carbon dioxide, this was offset by the dry reforming process. Gossler et al. reason that at high temperatures, the mixture proceeds towards chemical equilibrium, which amounts to a significant amount of syngas generation due to the endothermic nature of the reaction. During the expansion/cool-down phase, the equilibrium shifts away from the syngas side, however after a relatively small amount of time all reactions are quenched and the state from the “hot” equilibrium is mostly retained.

These aspects suggest that converting carbon dioxide contained in industrial off-gases, for example the main gases produced in the integrated steelmaking process or landfill gas, utilizing internal combustion engines is an interesting prospect and constitutes the subject matter of this work. As the internal combustion engine possesses many parameters that affect the reaction progression, a trial-and-error approach on an experimental basis is not practical. A modelling study however allows the relatively quick and wide-ranging analysis of the examined system. Therefore, a parameter study based on simulation is conducted to gain an overview of the viability of the idea and identify promising operating conditions that could then be validated using experiments.



## 2 Simulation details

### 2.1 Reactor model

The process of chemical transformation in an internal combustion engine was simulated using the DETCHEM<sup>ENGINE</sup> subpackage [10] of the DETCHEM program suite [11], which simulates a batch reactor with a variable volume profile. The reactions taken into account are based on a pure gas phase mechanism with no consideration for surface reactions. The program utilizes a single-zone model, meaning that the reactor volume is not spatially resolved. This type of model most closely resembles the performance of an HCCI (homogeneous charge compression ignition) engine. The system is described by the following differential equation system:

$$\frac{dn_i}{dt} = V \cdot \dot{\omega}_i, \quad (2.1)$$

$$\frac{dT}{dt} = \frac{\sum_i (\dot{n}_i \Delta H_i(T) - \dot{n}_i RT) - p\dot{V} - \dot{q}}{\bar{c}_V}, \quad (2.2)$$

where  $n_i$  is the amount of substance of species  $i$ ,  $t$  the time,  $V$  the reactor volume and  $\dot{\omega}_i$  the rate of formation of species  $i$ . The temperature is represented by  $T$ ,  $H$  signifies the molar enthalpy and  $p$  the internal pressure, while  $\dot{V}$  indicates the change in volume and  $\dot{q}$  the heat flux through the cylinder walls. Additionally,  $\bar{c}_V$  denotes the heat capacity of the gas at constant volume and  $R$  the ideal gas constant. Mole numbers, pressure, volume and temperature are linked by the ideal gas equation

$$pV = nRT. \quad (2.3)$$

The reactor volume is variable with respect to the crank angle and defined as:

$$V = V_c \left[ 1 + \frac{1}{2}(r_c - 1) \left( F + 1 - \sqrt{F^2 - \sin^2 \theta} - \cos \theta \right) \right], \quad (2.4)$$

where  $V_c$  indicates the clearance volume, which is the lowest reactor volume, reached at top dead center (TDC),  $r_c$  the compression ratio,  $\theta$  the crank angle, and  $F$  the ratio of

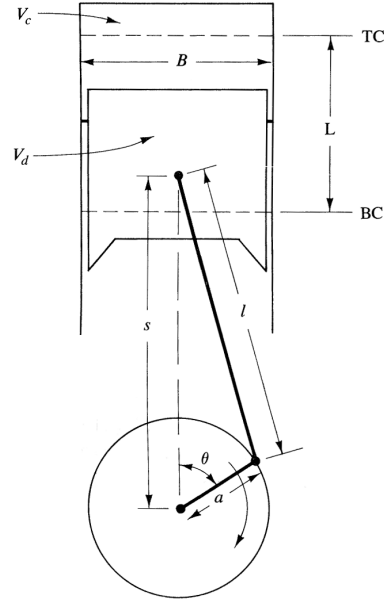


**Figure 2.1:** Geometric parameters in a schematic cylinder [12].

connecting rod  $l$  and crank radius  $a$ :

$$F = \frac{l}{a}. \quad (2.5)$$

These measurements are illustrated in a schematic cylinder in Fig. 2.1 along with the stroke  $L$ , bore  $B$ , and the displaced volume  $V_d$ .

The crank angle in turn depends on time and the engine speed

$$\theta = 2\pi Nt + \pi. \quad (2.6)$$

Concerning kinetics, the rate of formation of a species  $i$  is given by equation 2.7.

$$\dot{\omega}_i = \sum_j^{N_R} k_j \left[ (\nu''_{ij} - \nu'_{ij}) \prod_s^{N_S} c_s^{\nu_{sj}} \right] \quad (2.7)$$

The quantities  $N_R$  and  $N_S$  signify the number of reactions and species while  $k_j$  is the rate constant of the reaction  $j$ , while  $c_s$  is the concentration of species  $s$  in reaction  $j$ . Furthermore,  $\nu''_{ij}$  represents the stoichiometric coefficients of the products, and  $\nu'_{ij}$  those of the reactants of reaction  $j$ .

In this model, heat flux is described by the convective heat transfer to the cylinder walls:

$$\dot{q}(t) = h(t) \cdot A_{\text{total}}(t) \cdot \Delta T(t), \quad (2.8)$$

$$A_{\text{total}}(t) = A_{\text{piston}} + A_{\text{head}} + A_{\text{liner}}(t). \quad (2.9)$$

The temperature difference gas phase and cylinder wall is denoted by  $\Delta T$ , the total surface area of the reactor by  $A_{\text{total}}$ , which is comprised of the piston head, the cylinder head, and the round side wall, of which the area is time-dependent. Here,  $h$  is the heat transfer coefficient as defined by Woschni [13] to be a semi-empirical value, calculated by

$$h(t) = \alpha \cdot B^{-0.2} p(t)^{0.8} T(t)^{-0.53} w(t)^{0.8}. \quad (2.10)$$

The variable  $B$  represents the bore, the inner cylinder diameter, as the characteristic length for this system. The scaling factor  $\alpha$  was made out to be 99.6 via calibration of the pressure progression against an experiment where the given volume profile was applied to a nonreactive gas. The gas velocity  $w$  is calculated as follows:

$$w(t) = C_1 \bar{c}_{\text{piston}} + C_2 \frac{V_d T_0}{p_0 V_0} [p(t) - p_{\text{mot}}(t)]. \quad (2.11)$$

Here,  $C_1$  and  $C_2$  are constants (with values of 2.892 and  $3.24 \cdot 10^{-3} \text{ m s}^{-1} \text{ K}^{-1}$ , respectively),  $\bar{c}_{\text{piston}}$  is the mean velocity of the piston,  $V_d$  is the displaced volume and  $T_0$ ,  $p_0$ , and  $V_0$  are the initial values of temperature, pressure and volume. The term surrounded by brackets is meant to reflect the pressure conditions during combustion and consists of the difference in instantaneous pressure  $p(t)$  and  $p_{\text{mot}}(t)$ , the pressure existing during the compression of a nonreactive gas.

The DETCHEM<sup>ENGINE</sup> package is provided with the following parameters:

**Table 2.1:** DETCHEM<sup>ENGINE</sup> input parameters.

Parameter	Unit
Initial gas temperature	K
Initial pressure	Pa
Bore	m
Stroke	m
Compression ratio	-
Engine speed	s <sup>-1</sup>
Connecting rod length	m
Wall temperature	K
Woschni scaling factor	-
Mole fractions	-

These parameters, combined with the composition of the inlet gas, define the initial state and the volume profile of the system completely. The stroke is the distance between the points closest to (TDC) and furthest from (BDC, bottom dead center) the cylinder

head. The piston travels between these points. The engine speed is the number of revolutions performed by the engine per unit of time. The model only simulates a single compression-expansion step, equivalent to a single rotation. The connecting rod length is the length of the segment connecting the piston to the crankshaft, shown as  $l$  in Fig. 2.1.

### 2.1.1 Modeled systems

In this work, two real-world systems were simulated using the DETCHEM<sup>ENGINE</sup> code, a diesel engine and a rapid compression machine (RCM). The first system is a custom-fitted diesel truck engine (Volvo TD100) that was used for both simulation and experimental studies by Fiveland et al. [14] and used again for simulations utilizing the DETCHEM<sup>ENGINE</sup> code by Gossler [10]. The second modeled system is based on a rapid compression machine used previously to investigate the process of dry reforming of a methane/oxygen/carbon dioxide/argon mixture by Gossler et al. [9]. Rapid compression machines are commonly employed to study chemical processes under engine-like conditions [15]. The exact setup of this machine is described by Werler et al. [16] and Gossler et al. [9]. The geometric parameters of the modeled systems are listed in Table 2.2 along with the other parameters used for the simulations.

**Table 2.2:** Model parameters used for the simulations.

Parameter	Value		Unit
	Engine	RCM	
Bore	12.065	8.2	cm
Stroke	14	7.4	cm
Displaced volume	1.6	0.39	L
Compression ratio	19.8	8-12	-
Connecting rod length	26	26	cm
Initial temperature	462		K
Initial pressure	1		bar
Engine speed	10		s <sup>-1</sup>
Wall temperature	462		K
Woschni scaling factor	99.6		-

For reasons of simplicity, the general parameters, along with the geometric parameters of the Volvo engine, will be referred to as “standard operating conditions” in this work. The geometric parameters describing the RCM, with the compression ratio set to 10, combined with the general parameters, will from here on be referred to as “RCM conditions”.

## 2.2 Chemical model

The development of chemical kinetic models describing common chemical processes including combustion has been a major point of research during the latest decades, as the modeling of chemical systems became increasingly more common and accurate. As hydrocarbons represent the most common fuel type in general use, sophisticated mechanisms describing their combustion are abundant [17–25]. The GRI mechanism [26] is a widely-used chemical model focused on natural gas combustion in the gas phase and is therefore applicable to the system evaluated in this work. It has to be noted, however, that combustion is only one component of the reaction system at hand and dry reforming is the main focus of the performed studies. The mechanism consists of 325 reactions and 53 species in total and while all the species present in the considered primary gases are represented in the GRI mechanism, it was not specifically validated for dry reforming conditions. It has been validated for natural gas combustion against a number of experiments, including shock tube, flow reactor, and stirred reactor configurations and has been optimized for temperatures of 1000 K to 2500 K, pressures of 0.013 bar to 10.13 bar and equivalence ratios of 0.1 to 5. The conditions present in this case study however do not always reflect these conditions. While the temperature is in the denoted range during the combustion phase, the simulations predict pressures up to 30 bar due to the compression in addition to the temperature increase. Furthermore, the equivalence ratio of some mixtures that have been studied exceed the value of 5 that the GRI mechanism was optimized for.

Because of this, a new mechanism was developed specifically concerning methane combustion for the purpose of polygeneration by Porras et al [27]. Called PolyMech, it consists of 578 reactions among 90 species and contains elements of three separate mechanisms: The mechanism for  $\text{CH}_4$  combustion and pyrolysis by Hidaka et al. [23], the oxidation mechanism for  $\text{C}_1$ - $\text{C}_4$  species by Heghes [24] and the mechanism for the combustion of dimethyl ether (DME) by Zhao et al [25]. The mechanism also considers pyrolysis and oxidation reactions of acetylene [28], vinylacetylene [29], propyne and allene [30]. As polygeneration processes generally proceed at very fuel-rich compositions, the mechanism was validated against experimental data in these conditions and performed well [27, 31]. Additionally, the inclusion of dimethyl ether in the reaction scheme allows its evaluation as an ignition-enhancing additive. To study ozone for this same purpose, the PolyMech model was extended by a further 25 reactions with parameters from Starik et al. [32] and Howard and Finlayson-Pitts [33].

Both of these mechanisms were employed and are compared in Section 3.4.

## 2.3 Process workflow and automation

In order to simplify and accelerate the workflow, the software tool CaRMEN [34, 35] was implemented as an interface between the user and the DETCHEM program pack-

age. CaRMeN (Catalytic Reaction Mechanisms Network) is a tool designed to assist in comparing modeled and experimental results, automating and accelerating workflow as well as reducing human error and archiving data. Utilizing a custom driver, CaRMeN connects with the specific DETCHEM package (DETCHEM<sup>ENGINE</sup> for this work) and allows the execution of simulations selected from a graphical interface. Multiple simulation instructions are consolidated into one file, which allows CaRMeN to run a large amount of simulations with significantly less effort for the user than separately setting up each DETCHEM input file would require.

CaRMeN's fundamental application is the easy graphical depiction of semi-automated simulated and experimental data, making quick comparisons between various simulations or between simulations and experiments possible. A key feature allows the modification of a simulation with an additional list of parameters displayed in the interface, enabling a quick overview of the effect that parameter has on the calculated outcome. For example, a simulation of one engine cycle may be tested for a range of engine speeds with the results displayed in one graph. Including experimental data in this graph allows a judgement on which parameter creates the simulation matching the experiment most closely. This feature allows CaRMeN to be used for the validation of chemical or transport models amongst others.

CaRMeN also supports data pre- and post-processing through extension with user-written scripts, eliminating the need for additional calculations done by the user and thus limiting human errors. In this work, both data pre- and post-processing were utilized to enhance workflow and reduce the risk of errors caused by the amounts of repetitive calculations otherwise necessary. Pre-processing was extensively used for all simulations contained in this study. Due to the utilization of gas mixtures with fixed compositions (i.e. COG, BFG, air and LFG), the makeup of the gas fed to the engine is constrained to combinations of these primary gases. Since the DETCHEM<sup>ENGINE</sup> package takes mole fractions as the input for species amounts, calculating the exact composition of a secondary mixture is a tedious process and repeating it for every investigated mixture would take large amounts of time and possibly lead to user errors. Therefore, CaRMeN was extended by a script (also called loader) that reads the desired proportions of the primary gases in the CaRMeN input file and calculates the mole fractions of each species in the resulting mixture. This loader was later updated to enable the inclusion of two types of additives (see Section 3.5.4 on page 39) which are added to the secondary mixture. Post-processing was used to immediately calculate and display the conversion of CO<sub>2</sub> instead of its mole fraction, as the former is the quantity of interest for most studies performed in this work. This is achieved by CaRMeN reading the DETCHEM output file, performing a calculation as defined in a loader, and returning the results as new data for display in the graphical interface. The conversion is calculated by the following formula:

$$X_{\text{CO}_2} = 1 - \frac{n_{\text{CO}_2,\text{out}}}{n_{\text{CO}_2,\text{in}}} . \quad (2.12)$$

This formula includes carbon dioxide that is produced during an intermittent combustion process if some of the fuel is oxidized prior to dry reforming. This can result in negative values, signifying that more carbon dioxide is produced during combustion than is consumed during reforming.

A single simulation by DETCHEM<sup>ENGINE</sup> returns the volume, temperature, and species profiles as a function of time. CaRMeN can display one or more of these quantities in one graph for a quick visual feedback. To investigate the effects of different parameters on the results, for example the conversion of carbon dioxide, a large amount of simulations have to be run. CaRMeN, combined with a user-written loader, allows the automatic execution of multiple simulations and the depiction of their results in a common graph. As an example, the effect of the initial gas temperature on the conversion of CO<sub>2</sub> is to be investigated. Using a custom loader and given the desired parameter with minimum, maximum, and increment values specified in the input file, CaRMeN runs a simulation for each parameter value and consolidates the results into one graph of the simulation results (e.g. conversion) as a function of the parameter (e.g. initial temperature). This feature is not limited to physical parameters but can for example also be used to study the effects of different amounts of additives on the reforming process.

Taking advantage of this aspect, a semi-automatic optimization for more than one parameter can be performed using a modified version of the loader used for parameter studies. In the following work, this process was used to determine the composition of a mixture that would yield the highest conversion of carbon dioxide (see Section 3.5.2). To accomplish this, one parameter (e.g. the COG percentage) is chosen for a parameter series as mentioned above and the simulations are displayed in the graphical interface. The user can then visually identify a maximum or modify the parameter values until one is found. The parameter value corresponding to this maximum is then set as a constant and a new parameter (e.g. the BFG percentage) is chosen as the new variable parameter. This process is repeated with every optimization variable until the maximum value no longer increases significantly. This method will find a local maximum if there is one, but cannot guarantee that it will be a global maximum as well. Nonetheless, this is an extremely useful feature, as it enables an optimization which would not be possible using only the manual configuration of the simulation package and eliminates the need for an external optimization tool, which would require additional data conversion and transfer.



# 3 Results

## 3.1 General reaction observations

The main focus of this work is the conversion of  $\text{CO}_2$  from steelworks off-gases inside an internal combustion engine via dry reforming. These off-gases consist primarily of  $\text{CO}_2$ ,  $\text{CO}$ ,  $\text{CH}_4$ ,  $\text{H}_2$ ,  $\text{N}_2$ , and  $\text{H}_2\text{O}$ , with smaller amounts of larger hydrocarbons and argon. Due to the complex nature of these mixtures, many reaction pathways are possible and have to be considered. Figure 3.1 shows an exemplary species profile for a reaction mixture made up of COG, BFG and air under standard engine conditions, defined in Table 2.2 on page 8.

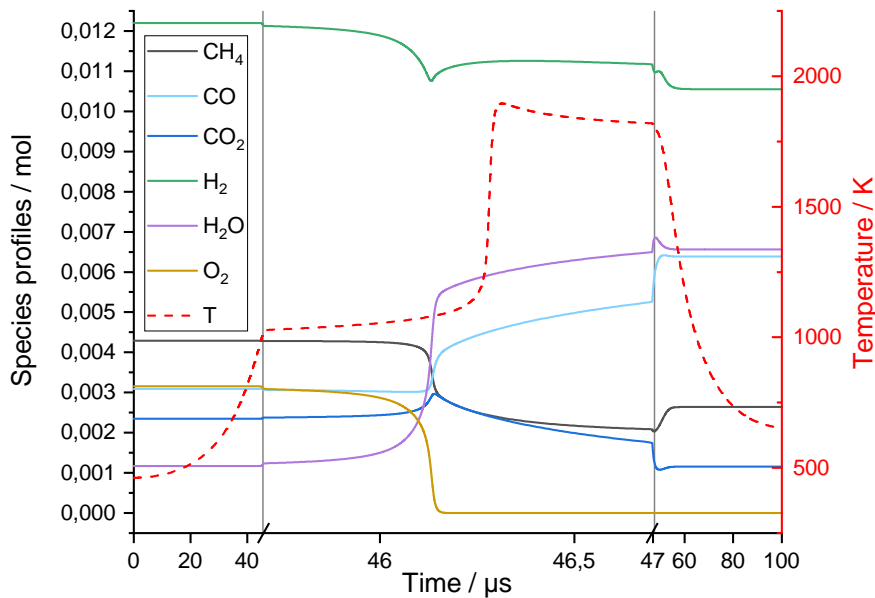
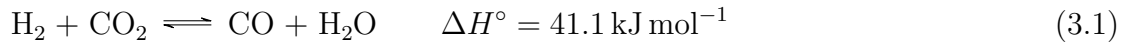


**Figure 3.1:** Species profiles of major relevant species around TDC (0.05s) during a simulation at standard operating conditions (listed in Table 2.2).

The species profiles show, in agreement with results found by Gossler et al. [9], that addition of oxygen (in this case air) enables the combustion of methane and hydrogen,

which leads to a spike in temperature. The combustion reaction is characterized by sharp drop in the  $\text{CH}_4$ ,  $\text{O}_2$  and  $\text{H}_2$  profiles, as well as a temporary increase in  $\text{CO}_2$ . The mole numbers of  $\text{CO}$  also increase, indicating that partial oxidation takes place in addition to the total oxidation of methane. As high temperatures are reached, the dry reforming reaction sets in. This is indicated by a continued drop in  $\text{CH}_4$  concentration along with a decrease in  $\text{CO}_2$ , with further generation of  $\text{CO}$ . The  $\text{H}_2$  profile increases briefly and then decreases slowly. This suggests that hydrogen is produced by dry reforming, but also consumed in another reaction, likely in the reverse water-gas shift reaction (Eq. 3.1), further converting  $\text{CO}_2$ .



This is supported by the species profiles of simulations that only included the two off-gases COG and BFG without any oxygen/air present, shown in Fig. 3.2. At low initial temperatures, the mole number of  $\text{CH}_4$  remains steady during compression, while those of  $\text{CO}_2$  and  $\text{H}_2$  decrease, indicating complete consumption via reverse water-gas shift. As the intake temperature increases, the focus shifts onto dry reforming. This is signified by a simultaneous decrease in  $\text{CH}_4$  and  $\text{CO}_2$  mole numbers, while the profile of  $\text{H}_2$  rises due to its generation in the dry reforming reaction.

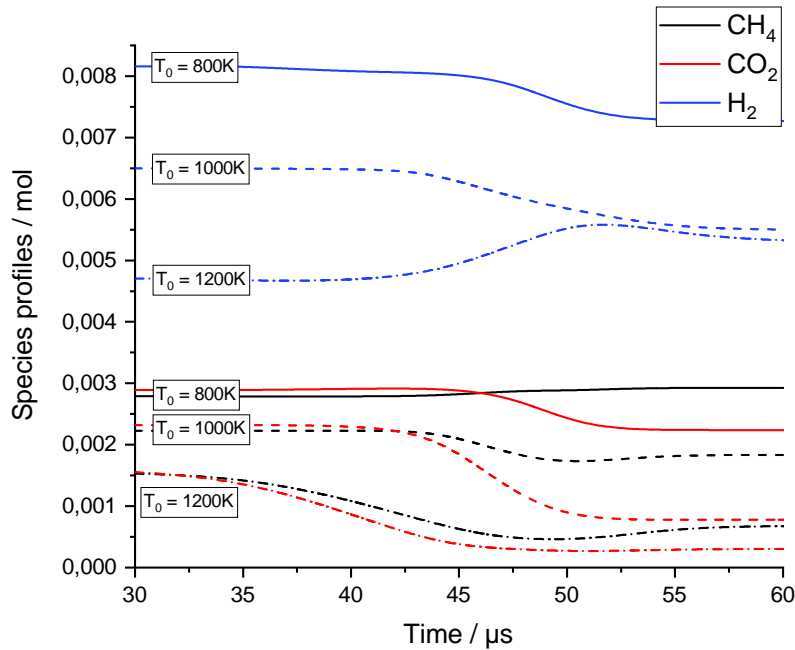


**Figure 3.2:** Species profiles for  $\text{CH}_4$ ,  $\text{H}_2$  and  $\text{CO}_2$  for three initial temperatures and a 1/1 mixture of COG and BFG.

For reactions that include oxygen, the temperatures reached by combustion reach values above 1800 K, leading to dry reforming being the prevalent follow-up reaction.

Generally, the product gas of this process consists of the same species as the intake gas, albeit in different amounts. The reforming of BFG using COG and air, which has shown to be a promising setup, produces a gas that is rich in syngas (between 35 % to 40 % for conversions around 50 %) with a H<sub>2</sub>/CO ratio of 1.5-2. The remaining part of the product is made up of inert N<sub>2</sub> (around 40 %), water (around 15 %), and remaining CH<sub>4</sub> (around 5 %) and CO<sub>2</sub> (<5 %). In the following, the effects of various geometric and operating parameters as well as the initial gas composition on the process inside the cylinder are evaluated. Concerning the H<sub>2</sub>/CO ratio, only extreme parameter values change this value drastically, for most parameter ranges and combinations the ratio remains between 1.5 and 2.

## 3.2 Effects of engine parameters on CO<sub>2</sub> conversion

To evaluate the validity of dry reforming of steelworks off-gases inside an internal combustion engine in general and identify operating conditions favorable to this process, the effect of various engine parameters on the conversion of carbon dioxide has been investigated. The DETCHEM<sup>ENGINE</sup> package contains 5 parameters only pertaining to the physical design of the engine and its operation. They are listed in Table 3.1.

**Table 3.1:** Engine parameters of the utilized DETCHEM<sup>ENGINE</sup> package.

engine parameter	unit
bore	m
stroke	m
engine speed	s <sup>-1</sup>
connecting rod length	m
compression ratio	-

These parameters were varied, using the Volvo engine described in Section 2.1.1 on page 8 as a baseline. The effects of these variations on the CO<sub>2</sub> conversion are laid out in the following. While one parameter was varied for each study, the others were kept constant at the standard operating conditions defined in Table 2.2. If not stated otherwise, the chemical model used for all simulations is the PolyMech mechanism, as it was specifically designed for polygeneration systems.

The gas composition used for these preliminary simulations was determined by a spot check for a composition with a high carbon dioxide conversion (about 50 %) in standard operating conditions. As the parameter study is primarily qualitative and intended to identify general trends, using the optimal gas composition is not strictly necessary. Additionally, the optimal composition is very dependent on the operating conditions

and would have had to be determined for every parameter value. As the optimization is done manually as detailed in Section 2.3 on page 9, the process is very time-consuming and was omitted for this evaluation. The gas composition used is comprised of coke oven gas, blast furnace gas, and air in a ratio of 2/1/1.5. The species mole fractions corresponding to this composition are listed in Table 3.2.

**Table 3.2:** Initial mole fractions (in %) for engine parameter studies, corresponding to a mixture of 2/1/1.5 (COG/BFG/air).

CH <sub>4</sub>	CO <sub>2</sub>	CO	H <sub>2</sub>	C <sub>2</sub> H <sub>4</sub>	O <sub>2</sub>	H <sub>2</sub> O	N <sub>2</sub>	Ar
9.78	5.35	7.04	27.8	0.889	7.19	2.67	39.0	0.32

#### 3.2.1 Connecting rod length

The effect of the connecting rod length at different temperatures was investigated and its effect on the conversion of CO<sub>2</sub> was found to be small. Even the variation of the rod length by  $\pm 60\%$  only yields a difference of less than 0.1% in conversion. Although the connecting rod length is directly represented in the formula for the volume profile of the modeled reaction chamber (equation 2.4), its influence is only marginal. Especially at the point of TDC, the profiles only differ slightly for different ratios of connecting rod length and crank radius [10], leading to a low dependence of conversion on the connecting rod length.

#### 3.2.2 Bore and stroke

Bore and stroke define the volume difference between the maximum and minimum volume during the engine cycle. Therefore, a correlation of the ongoing reaction with these parameters might be expected. It is common practice to combine these two parameters into a single number [36, 37], the stroke ratio  $\sigma$ , defined as

$$\sigma = \frac{B}{L}, \quad (3.2)$$

with  $B$  and  $L$  indicating the bore and stroke of the cylinder, respectively. If the bore and stroke of the configuration are equal, the engine is also referred to as square. Is the stroke larger than the bore, the engine may be referred to as long-stroke, otherwise as short-stroke. This quantity is widely used and will therefore be evaluated in place of separate studies into bore and stroke. Generally, increasing either bore or stroke with its counterpart set to a constant value will increase the conversion, as the displaced volume is increased. The displaced volume  $V_d$  is characterized by the volume of the cylinder the

piston head moves through:

$$V_d = \pi \left( \frac{B}{2} \right)^2 L. \quad (3.3)$$

To investigate the effect of the stroke ratio, its value is varied while keeping the displaced volume constant at 1.6 L. This is achieved by varying both the stroke and bore such that Equations 3.2 and 3.3 are fulfilled. The results of these simulations are depicted in Fig. 3.3 alongside the bore and stroke values for each stroke ratio.

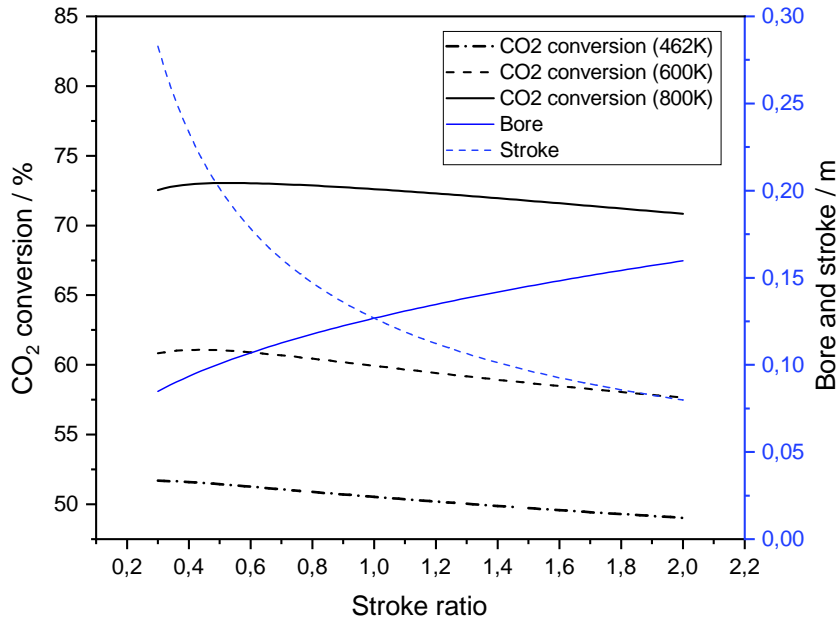


**Figure 3.3:** Effect of stroke ratio with a constant displaced volume of 1.6 L at atmospheric pressure, an engine speed of  $10 \text{ s}^{-1}$  (600 rpm), and a displaced volume of 1.6 L on CO<sub>2</sub> conversion. The conversions (black, left axis) for three initial temperatures and the values for bore and stroke (blue, right axis) are displayed for each stroke ratio.

The data show that employing a long-stroke engine leads to higher conversions, although the effect is not very pronounced, only impacting the conversion by about 5% over the entire span of stroke ratios, which includes all ratios used by commercially available engines. At higher initial temperatures a maximum, which moves to higher stroke ratios for increasing intake temperatures, is observed. Most commercial engines are close to square (i.e. with a stroke ratio of around 1), meaning their predicted conversions are within 3% to 5% of the maximum values in this respect.

### 3.2.3 Compression ratio

The compression ratio is a crucial parameter for the ignition characteristics and performance of any engine. It is defined as the ratio of maximum and minimum volumes during the engine cycle, calculated with the displaced volume  $V_d$  and the clearance volume  $V_c$ :

$$r_c = \frac{V_c + V_d}{V_c}. \quad (3.4)$$

It signifies the changes the contained gas undergoes in a relative form as opposed to the displaced volume, which relates only to the absolute change in volume. The simulated Volvo engine is an originally diesel-fueled engine and has a compression ratio of 19.8, a typical value for CI engines. Commercial spark ignition engines usually possess compression ratios of around 10. The effect of the compression ratio with constant stroke and bore is detailed in Fig. 3.4 for different initial temperatures.

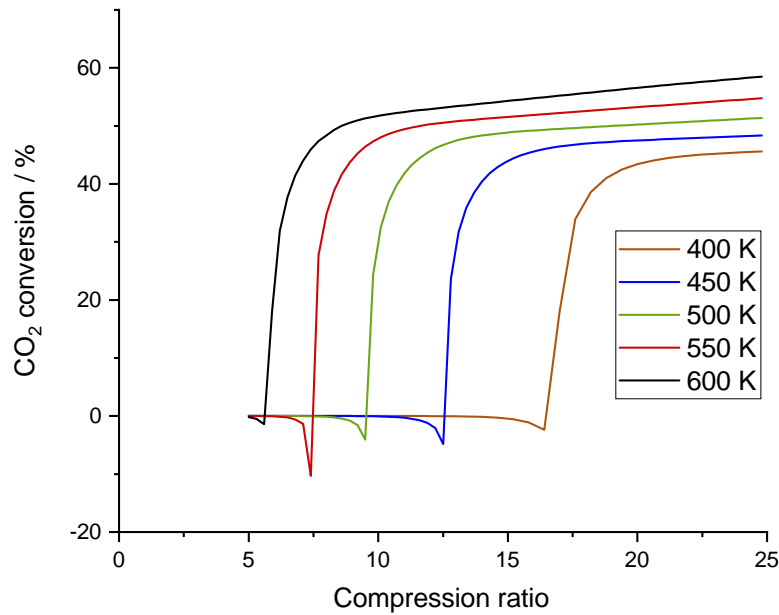


**Figure 3.4:** Effect of compression ratio on  $\text{CO}_2$  conversion for intake temperatures ranging from 400 K (brown) to 600 K (black). Other than for the compression ratio and the initial temperature, the standard operating conditions from from Table 2.2 were used.

As is evident from Fig. 3.4, the compression ratio has a major impact on the  $\text{CO}_2$  conversion and can also determine whether ignition occurs at all. Due to the fact that the compression ratio signifies the variation in volume of the system, it is linked to

the temperature of the gas mixture through the ideal gas law (Eq. 2.3). In fact, in an adiabatic reactor, the temperature would increase inversely proportional to the change in volume. However, in the model used by DETCHEM<sup>ENGINE</sup>, heat is lost through the cylinder walls, and the correlation is therefore not as straightforward. A higher compression ratio nevertheless leads to higher temperatures, which promote ignition. As shown in Fig. 3.4, for each temperature there exists a critical compression ratio above which ignition occurs. For example, the critical compression ratio for a gas that is injected at 500 K is about 10. But even after this minimum compression ratio the conversion rises further, as higher temperatures promote the endothermic dry reforming reaction and the equilibrium is shifted towards the product side.

Given that a higher compression ratio can induce ignition at lower initial gas temperatures, it is an important parameter for this process that can reduce energy consumption. The disadvantages to high compression ratios are effects on material stability and degradation. Higher pressures when working at high compression ratios contribute to material wear and thus reduce longevity. These drawbacks must be considered when higher compression ratios are desired.

#### 3.2.4 Engine speed

Engine speed is another important parameter to the engine operation, not only relevant for the singular reaction process but also when considering the larger operation due to its effect on system throughput. As one of the biggest advantages of the use of internal combustion engines for chemical synthesis, the engine speed is quickly adjustable to account for varying demands while also being variable over a large range. The effect of engine speed on CO<sub>2</sub> conversion is detailed in Fig. 3.5.

The behavior of conversion as a function of the engine speed is quite interesting, one might expect an increased engine speed causing higher temperatures because of the diminished impact of heat loss and therefore higher conversions. This effect is only noticeable at low engine speeds however, the position of the conversion maximum is dependent on the intake temperature and lies below 100 s<sup>-1</sup> (which corresponds to 3600 rpm) for the evaluated initial temperatures. For higher speeds, the conversions decrease because of ignition delay and the resulting non-completion of the reaction. The effect of ignition delay is especially noticeable in the higher range of engine speeds, as it results in negative conversions and an asymptotic behavior towards large values. The behavior in this section (the range of 100 s<sup>-1</sup> to 200 s<sup>-1</sup> for an intake temperature of 450 K) is explained by looking at the individual simulations that make up its data points.

In Fig. 3.6, the progression of temperature versus the crank angle is shown for different engine speeds from this range. Figure 3.7 shows the mole number evolution of two relevant species to this process, methane and carbon dioxide, for three engine speeds in the relevant range in the time frame around TDC (from 40 % to 70 % of total cycle duration). At lower temperatures (462 K in this example), the oxidation of a portion of

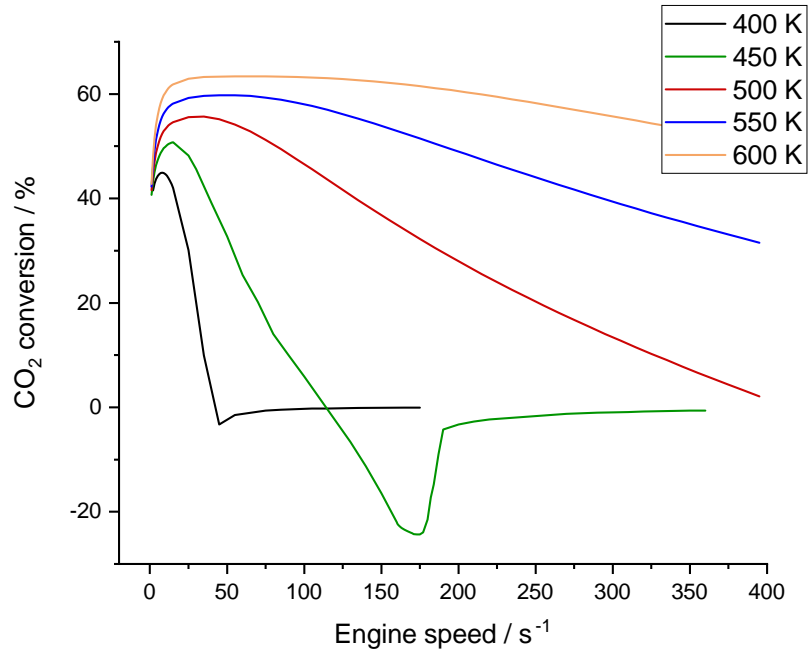


**Figure 3.5:** Effect of engine speed on  $\text{CO}_2$  conversion at various intake temperatures from 400 K to 600 K. Otherwise the standard conditions from Table 2.2 are used.

the fuel is needed to provide the temperatures necessary for dry reforming, compression alone would not lead to significant conversion of carbon dioxide. This reaction sets in first and features a large increase in temperature and a jump in species mole numbers, specifically the oxygen concentration dropping to zero. Figure 3.6 shows the transition from a sharp increase in temperature at TDC (at  $100 \text{ s}^{-1}$  / 6000 rpm) to a delayed, much softer increase at higher engine speeds (at  $177.4 \text{ s}^{-1}$  / 10 644 rpm), to a profile that resembles a non-reactive mixture (at  $190 \text{ s}^{-1}$  / 11 400 rpm). The behavior for an engine speed of  $100 \text{ s}^{-1}$  is exemplary for all profiles at slower speeds. The temperature and mole fraction behaviors follow the same pattern for each engine speed, while the values differ. For example, the mole fraction of  $\text{CO}_2$  after completion of the reaction increases with increasing speed as there is less time for the dry reforming reaction to take place. As a result of this the conversion decreases with increasing engine speed in the range from  $15 \text{ s}^{-1}$  to  $200 \text{ s}^{-1}$ . At around  $130 \text{ s}^{-1}$ ,  $\text{CO}_2$  is no longer consumed, but produced, as indicated by the negative conversions. At this point, combustion sets in so late that the following dry reforming reaction does not last long enough to be able to convert the amount of carbon dioxide generated by the prior oxidation.

To compare the point of ignition between simulations with different engine speeds, the point of maximum temperature, which is reached when the combustion of methane

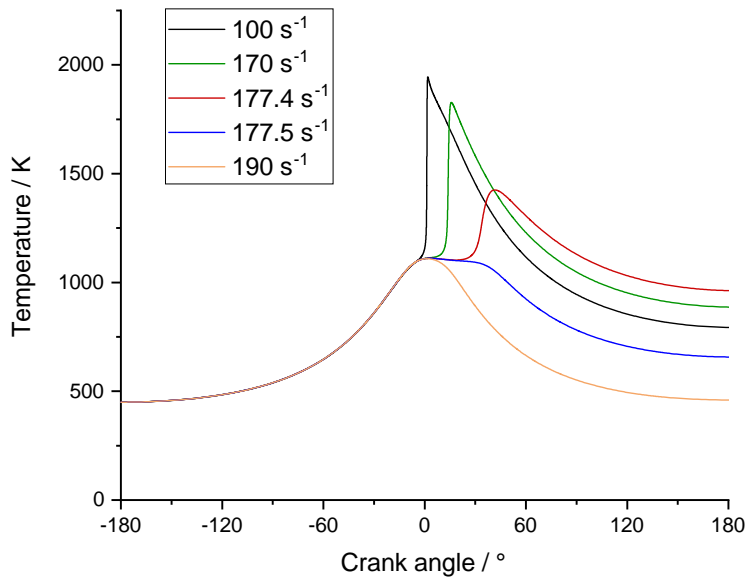


**Figure 3.6:** Temperature profiles during a single compression-expansion step at engine speeds from  $100\text{ s}^{-1}$  to  $190\text{ s}^{-1}$  (6000 rpm to 11 400 rpm), with an inlet temperature of 450 K.

has finished and all oxygen is consumed, is chosen as a reference. For  $100\text{ s}^{-1}$  this is the case at  $1.8^\circ$  after TDC, while at lower engine speeds the maximum is already reached during compression. Above an engine speed of  $100\text{ s}^{-1}$  the point of peak temperature is delayed more and more with increasing engine speed, as shown in Fig. 3.6. At  $177.4\text{ s}^{-1}$ , the peak temperature is only reached  $36^\circ$  after TDC.

Figures 3.6 and 3.7 shows that the ignition timing is significantly affected by engine speed. The ignition delay, however, can not be as easily defined in this engine configuration as for conventional spark or compression ignition engines. In a spark ignition (SI) engine, the ignition delay is defined as the time elapsed between the spark and the ignition of the fuel, denoted by a specific amount of change in some characteristic property, for example heat released or mass converted [38, 39]. In a compression ignition (CI) engine, the ignition delay is commonly defined as the time elapsed between fuel injection and the resulting auto-ignition. Both methods define a distinct point where the conditions allow for combustion, and measure the time therefrom to the point of actual ignition. This point is characterized by an already pressurized system and presence of fuel and oxidant in both types of engines. However, when operating the engine under HCCI conditions, the starting point for ignition delay is not as clear. The “injection point” in this case is bottom dead center, which is also the start of the simulation. This point is by definition also characterized by the inlet pressure and temperature, which

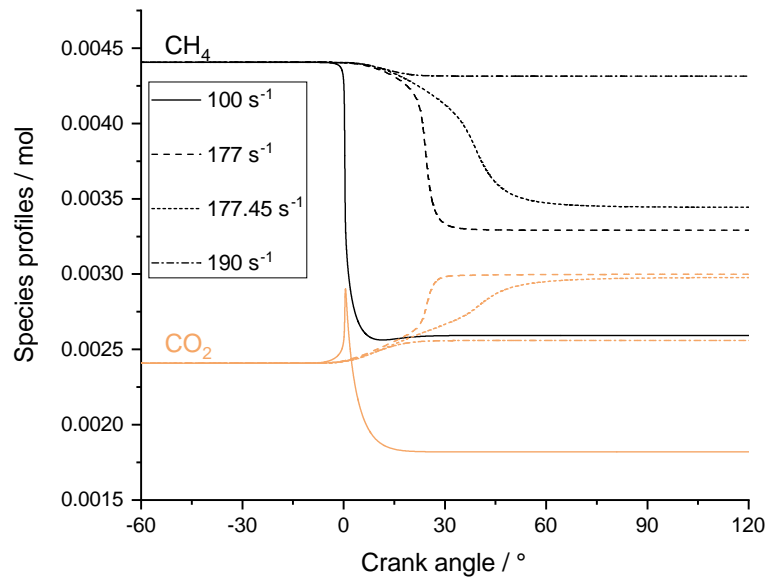


**Figure 3.7:** Species profiles of methane (black) and carbon dioxide (orange) during a single compression-expansion step at different engine speeds ranging from  $100\text{ s}^{-1}$  to  $190\text{ s}^{-1}$  (6000 rpm to 11 400 rpm).

for most initial conditions are not conducive to ignition. At TDC, there are conditions present that allow for ignition. Using TDC as a starting point however frequently leads to negative delays, which are physically meaningless, as ignition before TDC is quite common. Clearly, the first point allowing for ignition after a finite (or reasonable) amount of time must exist somewhere on the path from BDC to TDC, however, it is not trivial to find it and it will likely vary for different initial conditions. For this reason, TDC is chosen as a reference point for the discussion of ignition delay.

Considering this, looking at the species mole number development (figure 3.7) at an engine speed of  $100\text{ s}^{-1}$ , the successiveness of the two main global reactions is easily made out. At first, the methane is oxidized by oxygen, completely consuming the latter and producing carbon dioxide, increasing its concentration. Then, the remaining methane is able to reform part of the carbon dioxide, bringing it to a level slightly below its initial concentration. There is a rather sharp peak noticeable at  $0^\circ$ , indicating that the dry reforming reaction only becomes relevant when temperatures are already high. Further increasing the engine speed leads to negative values in conversions, signifying a net production of  $\text{CO}_2$ . At these speeds the dry reforming reaction is quenched so early that it does not consume more  $\text{CO}_2$  than was produced by the prior ignition step.

At an engine speed of  $170\text{ s}^{-1}$ , the point of peak temperature is already shifted by  $13^\circ$  compared to a speed of  $100\text{ s}^{-1}$ . The species evolution data in Fig. 3.7 show similarly

that the combustion of methane proceeds slower at these higher engine speeds. While methane has reacted completely within 10° of TDC at an engine speed of 100 s<sup>-1</sup>, at a speed of 170 s<sup>-1</sup> the reaction is completed by 36° past TDC. This behavior is not just caused by the fact that the piston retracts faster at higher engine speeds, the ignition delay is actually impacted by the engine speed as well. Relative to top dead center, the combustion of methane is completed after 0.3 μs at a speed of 100 s<sup>-1</sup>, while at 177 s<sup>-1</sup> oxygen is depleted after 0.7 μs. The oxidation reaction is clearly inhibited by higher engine speeds.

Figure 3.7 also shows that at this speed, not even the combustion of methane is completed before the system is “frozen” due to the expansion and associated pressure and temperature drop. This is the reason why less CO<sub>2</sub> is produced and the conversion is past its minimum in Fig. 3.5. After this minimum the CO<sub>2</sub> generation decreases and moves towards a limit at even higher speeds, which lies around -0.5%. The species profiles for engine speeds this high indicate that this minuscule generation of carbon dioxide is the result of the reaction of carbon monoxide with oxygen, both of which are present in the starting mixture.

The investigations into the effect of engine speed on conversion show that high speeds are actually detrimental to the consumption of carbon dioxide. However, it has also been shown that higher initial temperatures allow for the operation at much higher speeds. While higher intake temperatures require higher energy input, the predicted engine speeds achievable could increase the system throughput significantly. As an example, an initial temperature of 400 K attains a CO<sub>2</sub> conversion of 40% at 15 s<sup>-1</sup>, while an increase of 50 K enables the same level of conversion at 35 s<sup>-1</sup>, signifying a 133% increase in capacity.

#### Retention of valuable intermediates by engine speed manipulation

Another interesting effect of the engine speed is that it allows “freezing” of the gas composition at a specific point of reaction progress to obtain significant amounts of a specific product or interesting intermediates. For example, the simulations predict that during the dry reforming stage, significant amounts of acetylene (C<sub>2</sub>H<sub>2</sub>) are produced (more than 3 mol%), but consumed shortly thereafter. The engine speed can be adjusted in a way that the expansion/cool-down step that “freezes” the reaction mixture happens at the time where acetylene is present. While there may still be some consumption of this species, a significant proportion of it can be retained until the end of the process. This mechanism might enable the generation of significant amounts of valuable chemicals such as acetylene or formaldehyde and should be considered for further research. The behavior is demonstrated in Fig. 3.8.

It is also possible that this predicted concentration of acetylene will lead to soot generation inside the cylinder, as in practice, acetylene is a precursor to polycyclic aromatic hydrocarbons, which are nucleation sites for the formation of soot particles [40]. This reaction path is not featured in the utilized chemical models and cannot be easily

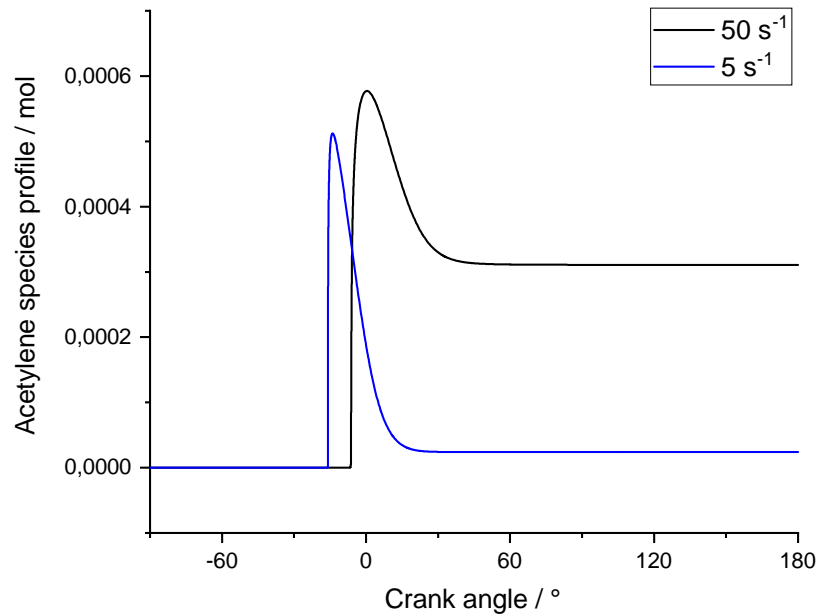


**Figure 3.8:** Species profile of acetylene at two engine speeds. At a low engine speed ( $5\text{ s}^{-1}$ , blue), it is both produced and consumed during the “hot” phase. At a speed of  $50\text{ s}^{-1}$ , a significant amount of it can be retained until the end of the process.

predicted without detailed mechanisms or experimental data. In a limited number of experiments under similar, very fuel-rich conditions during the studies presented by Gossler et al. [9] no soot development was observed. However, due to the frequent repetitions of engine cycles in an ICE, even minor soot formation can accumulate and potentially cause technical problems.

### 3.2.5 Wall temperature

During engine operation, the wall temperature is regulated via cooling on the outside of the cylinder. As heat retention is easier in stationary than in mobile engine applications, ideally most of the heat produced by the compression and reaction inside the cylinder is retained. However, without cooling, the engine will overheat, increasing material wear and possibly even damaging the setup. The effect of overheating has to be balanced against the positive effect of heat retention on the chemical processes inside the cylinder. To investigate these effects, the impact of the wall temperature on the  $\text{CO}_2$  conversion was studied. It is important to note that this temperature refers to the state of the inner cylinder wall, while in a real system, this value fluctuates and is regulated by the

temperature of the coolant. However, these fluctuations have shown to be small [41]. According to a study by Chang et al. [42], inner wall temperatures around 450 K are present inside an internal combustion engine and the standard wall temperature for this work was chosen as 462 K to account for the preheated intake gas. However, due to constraints in the potential application such as coolant evaporation and problems with materials of different thermal expansion coefficients, the operation at very high wall temperatures is of a rather theoretical nature.

The relation of wall temperature and carbon dioxide conversion is depicted in Fig. 3.9. As expected, a higher wall temperature leads to less heat loss and allows for higher temperatures and CO<sub>2</sub> conversions inside the reaction chamber. The effect is somewhat significant over smaller temperature ranges compared to other parameters. For example, at an engine speed of 20 s<sup>-1</sup>, going from a wall temperature of 300 to 500 K increases the CO<sub>2</sub> conversion by around 4%. Additionally, the simulations show that the wall temperature effect is different for low engine speeds, specifically at 5 s<sup>-1</sup>, compared to higher ones. At this low engine speed, the positive effect of wall temperature increases at higher values, while at higher speeds, the effect tapers off. The reason for this is the shortened residence time at higher engine speeds. A closer look at the species profiles for different wall temperatures shows that the main effect of a higher wall temperature is an earlier ignition of the fuel. This leads to a higher residence time in conditions conducive to dry reforming. At low engine speeds, this increase in reaction duration leads to an increase in the effect of wall temperature as it itself increases. At higher engine speeds however, the lower ignition delay matters less and less, as the dry reforming process is quenched earlier, explaining why the positive effect of a higher wall temperature tapers off.

During operation, the enhancement caused by higher wall temperatures (which would be realized by less cooling of the cylinder) has to be balanced against overheating of the engine, which can damage the setup. Additionally, in a stationary setup the heat transferred will be able to be reused partially, for example to preheat the intake gas.

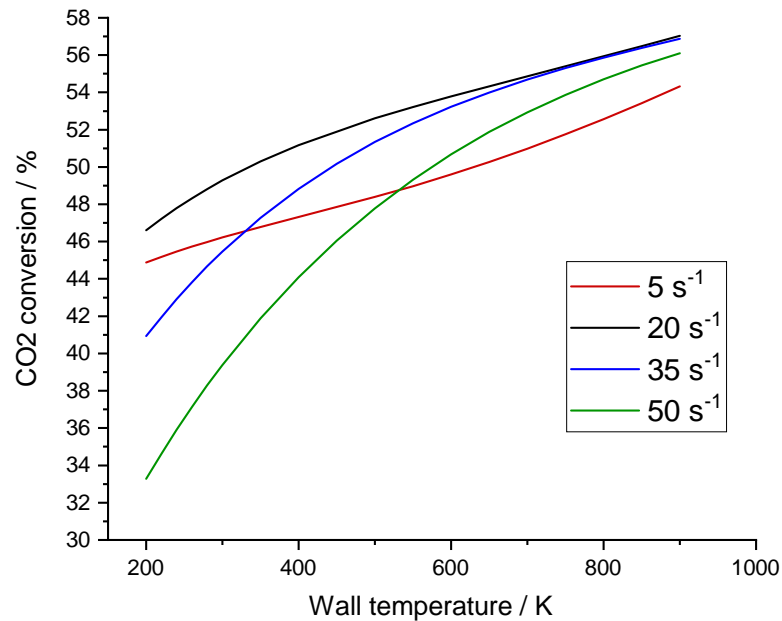


**Figure 3.9:** Effect of wall temperature on CO<sub>2</sub> conversion at engine speeds ranging from 5 s<sup>-1</sup> to 50 s<sup>-1</sup> (300 rpm to 3000 rpm). With the exception of the wall temperature, the standard conditions from Table 2.2 are applied.

### 3.3 Effects of inlet conditions

#### 3.3.1 Initial temperature

The initial gas intake of the internal combustion engine is characterized by two parameters apart from its composition in the DETCHEM<sup>ENGINE</sup> package, temperature and pressure. Via the ideal gas equation these also determine the total mole number of all species. While the three considered off-gases emerge from their respective sources at high temperatures, they are cleaned to remove potentially corrosive trace gases such as ammonia or hydrogen sulfide [43]. During this cleaning process, the gases are cooled down to near room temperature [5, 43]. While it may be possible for some of these gases to be utilized before cleaning because of the general chemical stability of engines made of cast iron and an absence of catalysts that may be poisoned by traces such as hydrogen sulfide, the primary gases are considered to be present at ambient conditions (298 K and 1 bar). Therefore, lower initial temperatures and pressures are economically desirable as they decrease energy needs. The effect of the initial gas temperature on the CO<sub>2</sub> conversion is shown in Fig. 3.10.

For this simulation series, the GRI mechanism was used, as it is more stable and

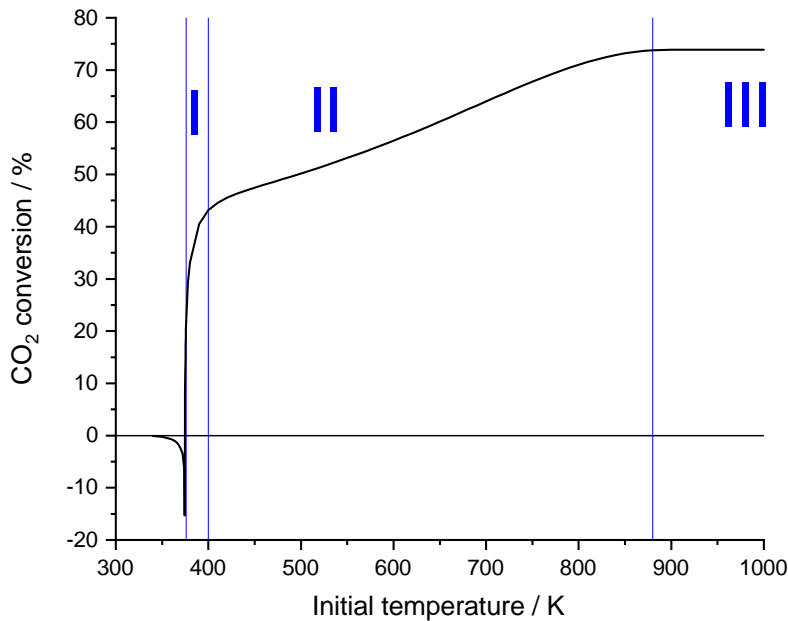


**Figure 3.10:** CO<sub>2</sub> conversion as a function of initial gas temperature, divided into three regions. Apart from the initial temperature, the standard conditions (see Table 2.2) are used.

was able to simulate the process at lower temperatures, where the PolyMech mechanism failed to do so. However, while the conversions differ slightly (a more detailed comparison is found in Section 3.4), the general behaviors at higher temperatures are the same.

Clearly there is a positive correlation between initial gas temperature and conversion, however the exact behavior is quite peculiar. As the conversion of CO<sub>2</sub> at lower temperatures heavily depends on the fact whether ignition occurs, the lowest initial temperature leading to autoignition is a relevant quantity and will be studied for different conditions in this work. For clarity, this temperature will be referred to as “ignition temperature”, with ignition being characterized by a rapid and significant increase in temperature. For this mixture and initial parameters the ignition temperature is 376 K.

Below this temperature, ignition does not occur, however minor amounts of methane and carbon monoxide are oxidized to carbon dioxide, resulting in small negative conversions. The behavior above the ignition temperature can be broken up into three regions: At first the conversions increases rapidly with respect to temperature, while it only increases slowly after about 400 K. After a certain temperature (870 K in this case), the conversion no longer increases with initial temperature. The reason for the first change in behavior lies in the temperature present after the initial methane combustion. To illustrate the reason for this behavior, the temperature developments for three intake

temperatures in the first and three in the second region are shown in Fig. 3.11. For each region, the initial temperatures chosen were 1 K apart.

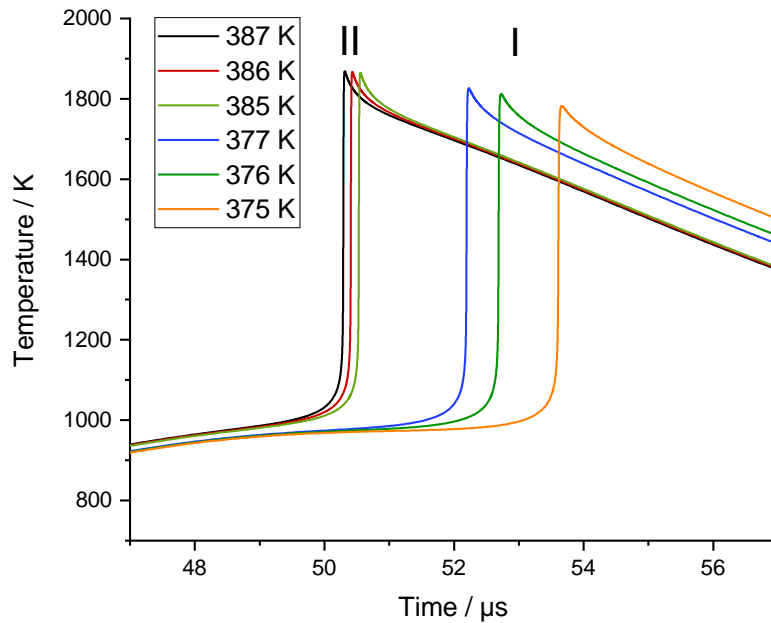


**Figure 3.11:** Comparison of temperature profiles around TDC for three temperatures each in regions I (375 K to 377 K, right) and II (385 K to 387 K, left).

As the figure shows, the difference in ignition timing and the temperature is much greater between simulations in the first region than in the second, even though the difference in initial temperature is 1 K for each triplet of values. While in the first region, peak temperatures range from 1780 K to 1830 K, temperatures of 1865 K to 1867 K are reached in the second. The increased temperatures in the second region favor the dry reforming reaction and result in higher  $\text{CO}_2$  conversions. The higher difference in peak temperatures also causes the simulations from the first region to predict quite different conversions (12.2%, 21.7% and 26.3%, respectively), while the three initial temperatures in the second result in similar values (between 38% to 39%). This is confirmed by closer inspection of the species profiles of carbon dioxide, as its rate of consumption is noticeably larger at an intake temperature of 377 K than at 375 K, while the quenching of the reaction happens at similar times. The differences in ignition delay also lead to slightly longer residence times in hot conditions, contributing to this discrepancy between conversions to a smaller extent.

The reason for the plateau of  $\text{CO}_2$  conversion above 870 K is that at temperatures this high all methane present in the initial mixture is depleted by either the oxidation

or the dry reforming reaction, meaning the maximum conversion is reached. This is illustrated in Fig. 3.12 by the developments of the species profiles of methane and carbon dioxide over time. The intake mixture contains COG, BFG and air in a 2/1/1.5 ratio, corresponding to the mole fractions laid out in Table 3.2 on page 16. The simulation predicts that an initial temperature of 700 K is not enough to result in the full conversion of methane. At an initial temperature of 900 K, however, ignition occurs after 28 ms (corresponding to compression by a factor of 2) and methane is already depleted before TDC is reached at 50  $\mu$ s.

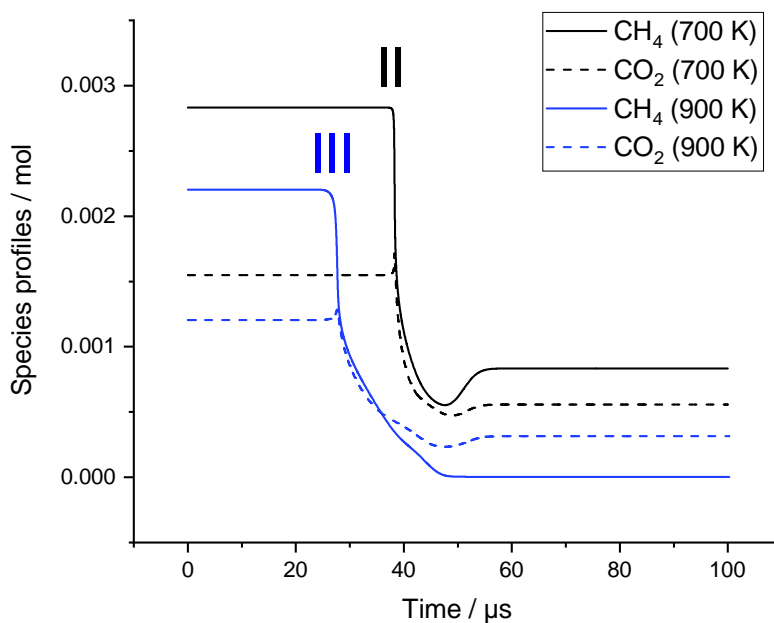


**Figure 3.12:** Comparison of species profiles for methane (solid) and carbon dioxide (dashed) for initial temperatures in regions II (700 K, black) and III (900 K, blue).

### 3.3.2 Initial pressure

While the considered steelworks off-gases are produced at atmospheric pressure [44], the initial pressure is another parameter that is easily adjustable via the use of a compressor. Purely from a process standpoint, higher pressures allow for higher system capacities, which reduces the number of reactors necessary at a constant mass flow.

The pressure dependence of conversion is therefore investigated and shown in Fig. 3.13 in the range of 0.02 bar to 5 bar. As in Section 3.3.1, the GRI mechanism is used in this study for numerical stability.

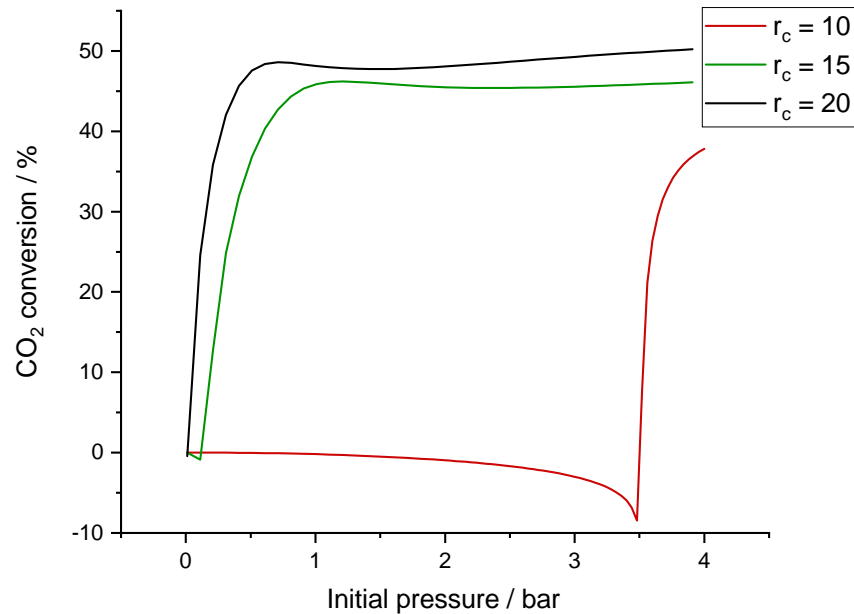


**Figure 3.13:** Effect of initial pressure on conversion for three compression ratios (10 (value for a common SI engine, red), 15 (green), and 20 (value for a common CI engine, black)).

The simulations predict that a pressure of 0.04 bar is enough to induce ignition and convert carbon dioxide at the typical compression ratio of 20. In fact, closer evaluations reveal that even at a pressure of 0.05 bar, 15 % of carbon dioxide is converted, although pressures this small do not constitute any advantage to this process and are not relevant for practical discussion. The behavior of conversion as a function of pressure also shows that atmospheric pressure is enough to obtain a high conversion, while further increase in pressure will not impact it in a major way. Higher initial pressures may nevertheless still be considered, as the throughput of the system can be increased at the cost of using a compressor while not decreasing chemical efficiency. Interestingly, the simulations show a minimum in conversion at 1.50 bar. This phenomenon does not occur when employing the PolyMech mechanism, therefore it might be a result of certain pressure-dependent reactions in GRI.

### 3.4 Effect of the employed reaction mechanism

Two chemical models were used for the simulation of the in-cylinder processes, the GRI mechanism [26] and the PolyMech mechanism specifically created for the description of

polygeneration systems [27]. This allowed the evaluation of the two models against each other, which is featured in this section.

As the ignition temperature (term introduced in Section 3.3.1) is a practically important and characteristic quantity useful for the comparison of different parameter sets, the effect of the employed mechanism on this value was investigated. The mechanisms were compared for the dry reforming in two mixtures, one containing blast furnace gas and one containing basic oxygen furnace gas. Both mixtures are composed of two parts coke oven gas, one part BFG/BOFG, and 1.5 parts air. These simulations used the parameters of the RCM setup as the PolyMech mechanism did not provide consistently successful simulations at the low initial temperatures that allow for ignition in the diesel engine setup. The results are displayed in Fig. 3.14.

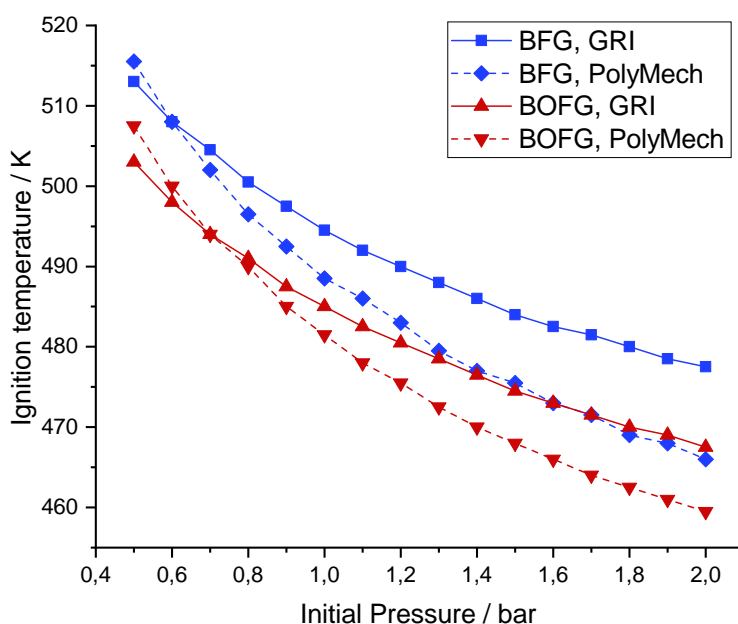


**Figure 3.14:** Effect of the implemented mechanism (GRI, solid and PolyMech, dashed) on ignition temperature for two gas mixtures. These mixtures have compositions of 2/1/1.5 (COG/X/air, with X being BFG (blue) or BOFG (red)) as a function of initial pressure.

This comparison shows that the choice of mechanism has a noticeable effect on the predicted reaction process. At initial pressures below atmospheric conditions, the chemical models agree somewhat regarding the ignition temperature. With increasing initial pressure however, the ignition temperature predicted by the PolyMech model decreases significantly faster. This leads to differences of as much as 10 K at initial pressures of

2 bar. The simulations in this work set an initial pressure of 1 bar, where the difference between the mechanisms is however not as high.

The effect of the selected mechanism on the CO<sub>2</sub> conversion as a function of temperature is shown in Fig. 3.15. The graph shows that using the PolyMech model leads to slightly higher predicted conversions for all temperatures until the plateau where the conversion cannot increase further (see Section 3.3.1 on page 26) is reached.

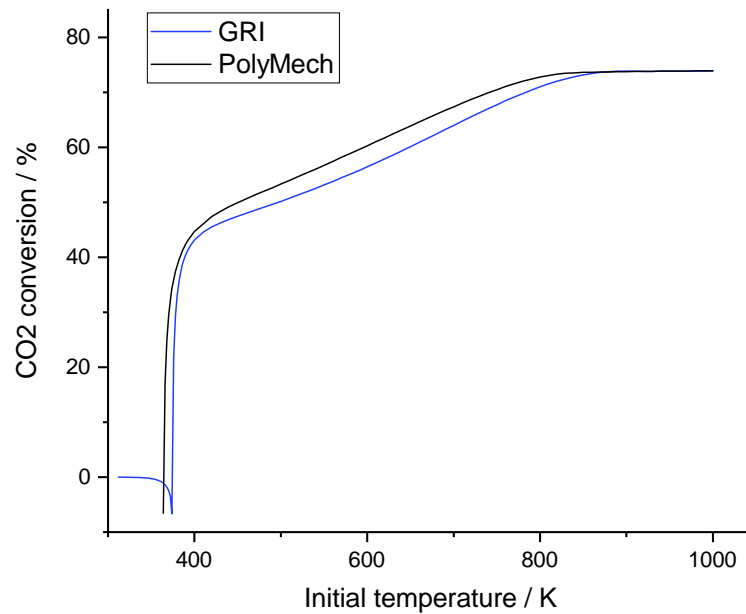


**Figure 3.15:** Comparison of CO<sub>2</sub> conversions as a function of initial temperature when employing the GRI (blue) and the PolyMech (black) mechanisms.

To determine which mechanism is better suited to approximate the studied systems, both should ideally be validated against experimental results of the RCM or the modified diesel engine. Additionally, even though the simulations are intended to model an engine in HCCI mode, the use of a single zone model is a simplification and the use of multi-zone models could improve results if experimental validation deems this necessary.

## 3.5 Effect of the gas composition

### 3.5.1 Primary gas proportions

The only initial parameter for the simulation left to be discussed is the chemical composition of the feed gas, certainly crucial to the process. As this study intends to model

the actual conversion of steelworks off-gases, the initial composition in the reactor is bound to be a combination of the gases available from a typical steel plant, which are listed in Table 1.1, and air.

**Table 3.3:** Compositions (in %) used for the three main steelwork off-gases [5] and air

	COG	BFG	BOFG	air
CO <sub>2</sub>	1.2	21.6	20.0	0.04
CO	4.1	23.5	54.0	0.0
H <sub>2</sub>	60.7	3.7	3.2	0.0
CH <sub>4</sub>	22.0	0.0	0.0	0.0
C <sub>2</sub> H <sub>4</sub>	2.0	0.0	0.0	0.0
N <sub>2</sub>	5.8	46.6	43.8	78.1
H <sub>2</sub> O	4.0	4.0	4.0	0.0
O <sub>2</sub>	0.2	0.6	0.7	20.9
Ar	0.2	0.6	0.7	0.96

Because of the stoichiometry of the dry reforming reaction,



the presence of both methane and carbon dioxide is strictly necessary. As shown in the table, coke oven gas (COG) is the only gas that contains methane, making it indispensable for this process. One of the other off-gases must also be included in the feed gas, as COG contains too little CO<sub>2</sub> to render the process viable. Blast furnace gas (BFG) has by far the highest volumetric output of the three off-gases with a volumetric flow rate of 730 000 Nm<sup>3</sup>/h for a model steel plant producing 6 Mt of steel per year [5]. Although basic oxygen furnace gas (BOFG) contains similar amounts of CO<sub>2</sub> as BFG, a much smaller quantity of it (35 000 Nm<sup>3</sup>/h) is produced in a steel plant, which makes its conversion less critical for emission control. Air is also included in the mixture to allow for the combustion of some of the fuel, leading to higher temperatures which are favorable for the endothermic dry reforming reaction. To evaluate the effect of the specific gas composition on the CO<sub>2</sub> conversion, some exemplary primary gas proportions were selected and investigated over a range of temperatures. The results are shown in Fig. 3.16.

These samples show some general trends concerning the gas composition. As noted above, the conversion of some mixtures will plateau at higher temperatures as all available methane is used up and no further carbon dioxide can be converted. This is caused by their smaller proportions of COG. On the other hand, if too much air is included in the mixture, too much methane undergoes complete oxidation and produces CO<sub>2</sub> instead of reacting with it in the dry reforming reaction, causing negative conversions.

Generally, less blast furnace gas or basic oxygen furnace gas result in higher conversions, although potentially at the cost of the absolute system throughput, as the mole

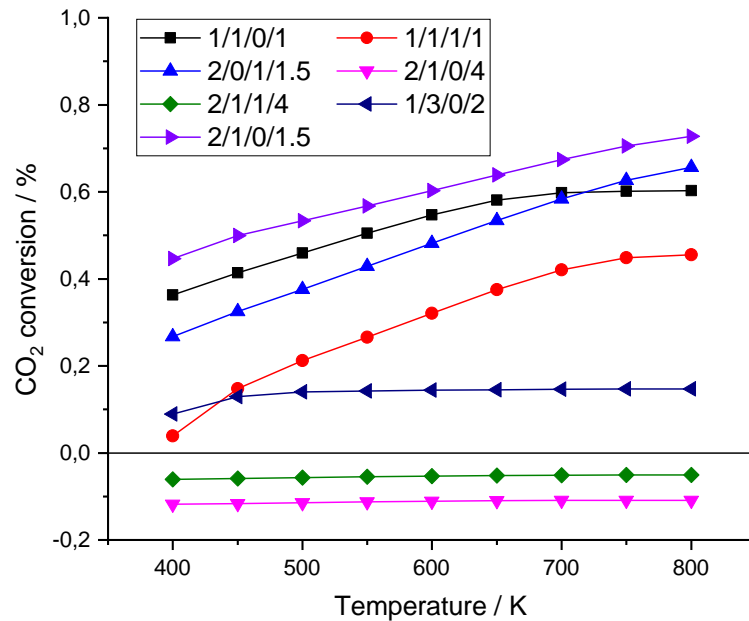


**Figure 3.16:** Comparison of  $\text{CO}_2$  conversions for multiple primary gas compositions (denoted by their composition of COG/BFG/BOFG/air) over a range of initial temperatures.

fraction of  $\text{CO}_2$  decreases with lower BFG and BOFG proportions.

### 3.5.2 Optimization of the gas composition

The gas composition was optimized semi-manually for the Volvo engine conditions by repeatedly simulating data series with the percentage of one of the four primary gases as a parameter. Initially, the proportion of one primary gas (e.g. COG) was varied and the conversion maximum identified. The gas percentage corresponding to that maximum was then kept constant and another primary gas proportion was chosen as the new parameter. This was continued until no variation of any gas share led to an increase in conversion of more than 0.1%. To limit the possibility that only a local maximum of the conversion was found, the optimization for the first initial temperature was started from four different starting points. All of these four optimizations led to the same result of optimal primary gas proportions for standard operating conditions of 2.49/0.63/1.39 (COG/BFG/air, corresponding to 55.2, 14.0, and 30.8%), yielding a conversion of 54.21%. Basic oxygen furnace gas is not represented in this optimal mixture. Any simulated series with its percentage as the variable parameter has its maximum at zero, meaning any addition of BOFG to a COG/BFG/air mixture leads to

a decrease in conversion. The major difference between the two CO<sub>2</sub>-containing gases is the presence of more carbon monoxide in BOFG in place of inert nitrogen in BFG. Closer inspection of the species profiles during a combustion/reforming process reveals that replacing BFG with BOFG leads to no relevant change in methane consumption. However, after the initial combustion the increase in concentrations of hydrogen and carbon dioxide are higher for mixtures containing BOFG, while the increase in carbon monoxide and water is less pronounced. This is shown in Fig. 3.17.

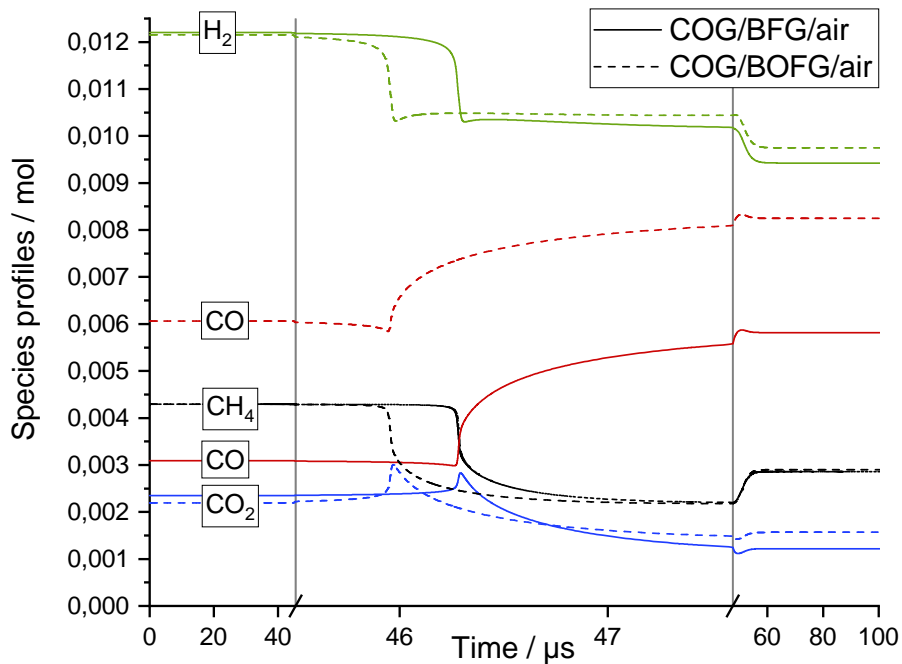
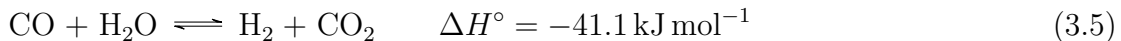


**Figure 3.17:** Species profiles for the reforming of 2/1/1.5 mixtures of COG/X/air, with X representing BFG (solid) or BOFG (dashed).

This suggests that the additional carbon monoxide contained in basic oxygen furnace gas increases the impact of the water gas shift reaction:



The increased relevance of this reaction leads to more CO<sub>2</sub> being produced and thus to reduced conversions. Another interesting point illustrated in the figure is that while the reforming of CO<sub>2</sub> is less pronounced, the ignition actually occurs earlier for the mixture containing BOFG. A possible reason for this is that the additional CO plays a larger

role in the mechanism leading to ignition than nitrogen, as it can take on or give off an oxygen radical, facilitating the chain reaction necessary for ignition. Because of the detrimental impact of the water-gas shift reaction, the optimization of any gas mixture containing both BFG and BOFG will reduce the latter's percentage until it reaches zero. To investigate the conversion of BOFG, a separate optimization was performed where the percentage of BFG was fixed at zero. This optimization produced a result of 2/0/0.35/1 (COG/BFG/BOFG/air) as the ideal composition for converting the carbon dioxide in BOFG under standard operating conditions, with a conversion of 41.48 %, a significantly lower value when compared to a COG/BFG/air mixture. Clearly the conversion of BOFG, even for the ideal composition, is less efficient than the reforming of a COG/BFG/air mixture. As the amount of BOFG produced in a typical steel plant is also much lower than that of BFG, the conversion of blast furnace gas should be the main focus over the regeneration of BOFG.

#### Optimized gas compositions as a function of temperature

To see how the CO<sub>2</sub> conversion increases with temperature, taking the change of the ideal composition into account, the optimal gas compositions for higher temperatures were also determined. The composition optimized in the previous section was used as the starting point for the optimization at the first temperature, and from then on the last result was used as the new starting composition. The optimal proportions of the primary gases and the conversions as a function of temperature are detailed in Fig. 3.18.

These data show that the CO<sub>2</sub> conversion can reach higher levels than the previous simulations (e.g. Fig. 3.10) have determined, with conversion levels of above 90 %, but at the cost of the use of more methane-containing and less-CO<sub>2</sub>-containing COG. This decreases the absolute amount of carbon dioxide that can be converted, as less BFG is present in the initial mixture. To illustrate this relation, the absolute amount of CO<sub>2</sub> converted is shown in Fig. 3.18 as a solid blue line. This absolute  $Y$  essentially denotes the percentage of molecules in the initial mixture which are CO<sub>2</sub> molecules that will be converted by the end of the engine cycle and is calculated by

$$Y_{\text{CO}_2} = X_{\text{CO}_2} * \sum_i Z_i * x_{i,\text{CO}_2}. \quad (3.6)$$

Here,  $X$  represents the conversion,  $Z$  the percentage of the primary gas  $i$  of the full mixture and  $x$  the mole fraction of CO<sub>2</sub> in the respective primary gas. Its maximum lies at a temperature of 740 K, where the total CO<sub>2</sub> converted is 2 %, corresponding to 72% of initial carbon dioxide being reduced.

#### 3.5.3 CO<sub>2</sub> conversion without prior methane combustion

In the simulations discussed above, air was added to the steelworks off-gases to enable methane combustion, providing the necessary conditions for the strongly endothermic

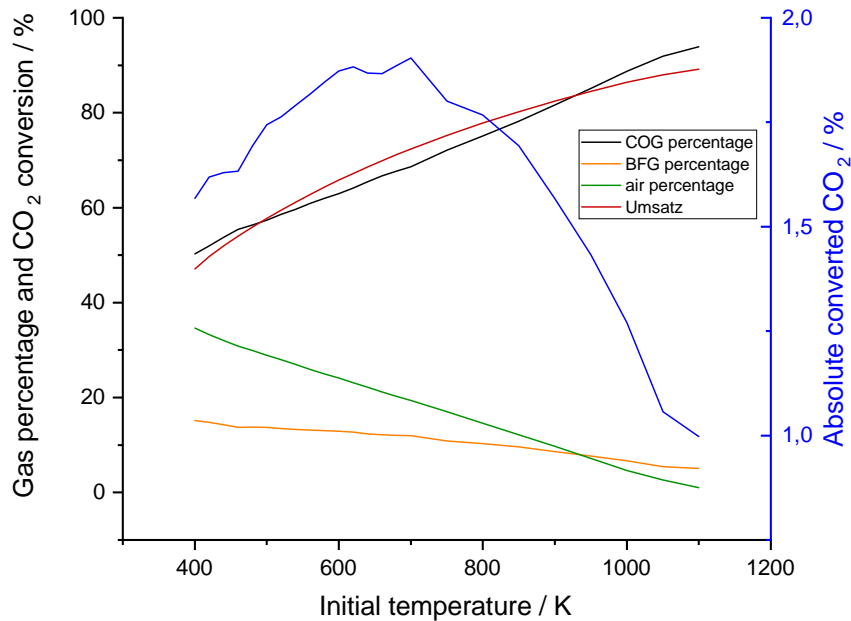


**Figure 3.18:** Optimal gas compositions (primary gas percentages on left axis, red, green and yellow) and the resulting conversions (black, also left axis) as a function of initial temperatures along with total converted CO<sub>2</sub> in blue (right axis).

dry reforming reaction to occur. However, methane combustion produces carbon dioxide and counteracts the ultimate objective of this process which is the reduction of greenhouse gas emissions. Therefore, pure reforming without the addition of air at higher temperatures is investigated. As shown in the general reaction discussion (Section 3.1 on page 13), at low initial temperatures, CO<sub>2</sub> is completely converted via the reverse water-gas shift reaction. Only at temperatures above 1000 K does the dry reforming reaction become relevant. Figure 3.19 shows the comparison of multiple COG/BFG mixtures in respect to their CO<sub>2</sub> conversions as a function of temperature. To illustrate and compare the compositions of these mixtures, Fig. 3.20 details the mole fractions for the most important species in each mixture. Figure 3.19 also shows the total amount of CO<sub>2</sub> converted as defined above for the investigated compositions.

The graph shows that while the ideal composition (in terms of conversion) of an airless mixture is very COG-rich, the temperature at which significant amounts of conversion occur are not much different at varied COG/BFG ratios. For example, a conversion of 40% is reached within 50 K for most compositions, covering a large range of COG/BFG ratios (7/1 to 1/3). Solely BFG-rich mixtures reach significant conversions only at much higher temperatures. As there is no oxygen available, there is no combustion step and

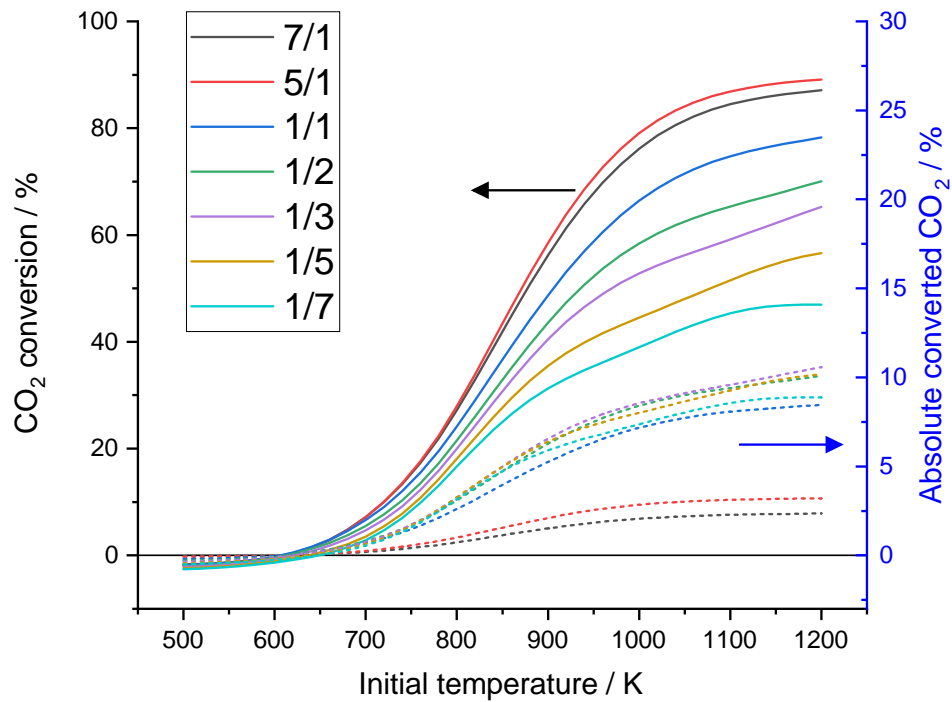


**Figure 3.19:** CO<sub>2</sub> conversions (solid, left axis) and total amounts of CO<sub>2</sub> converted (dashed, right axis) for various COG/BFG compositions ranging from 7/1 to 1/7 as functions of temperature.

therefore no initial temperature above which the conversion increases from negative to significant values as seen for flammable mixtures. The conversions therefore only increase slowly at first, but temperatures above 800 K allow for conversions comparable to those achieved with air included in the mixture. At high temperatures, the conversion levels differ much more strongly for different initial compositions than at lower temperatures. Nonetheless, Fig. 3.19 shows that the higher temperatures allow for the mixture to be more BFG-rich, improving the total consumption of carbon dioxide (shown as solid lines). While the “richer” (in terms of methane, as it is considered the fuel) mixtures have the highest conversions, due to the low amount of BFG, the absolute amount of converted carbon dioxide is the lowest. The ideal composition in terms of absolute conversion of CO<sub>2</sub> lies around 1/3 COG/BFG, which is far “leaner” than previously optimized mixtures containing oxygen. This composition allows an absolute conversion of around 6.55 % of carbon dioxide in the initial mixture at 900 K, which is more than three times the value reached using an air-containing mixture. The relative CO<sub>2</sub> conversion, however, is only around 40 %. This emphasizes the effect of an initial combustion step,

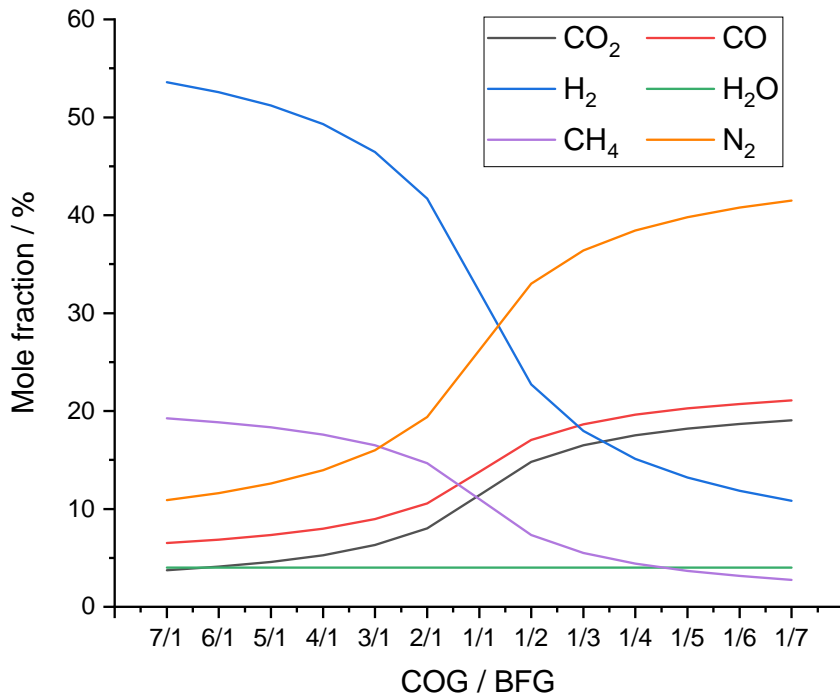


**Figure 3.20:** Compositions for the mixtures investigated and listed in Fig. 3.19. Only species with mole fractions above 2% are shown in this figure.

as temperatures of above 800 K are required to achieve conversions close to 50%, which are obtained below 500 K using mixtures containing air.

### 3.5.4 Effect of additives on ignition temperature and conversion

To allow dry reforming of the considered off-gas mixtures at low initial temperatures, part of the fuel can be oxidized as shown previously. Finding the lowest temperature at which a given composition ignites or attains a significant amount of CO<sub>2</sub> conversion is crucial to making the process energetically and economically viable. Therefore, the potential improvement that ignition enhancers can deliver is an important aspect to consider. Three such enhancers (dimethyl ether, hydrogen peroxide and ozone) were selected and evaluated with respect to their effect on initial temperature required for ignition and carbon dioxide conversion. These studies were simulated using RCM parameters to make validation of these findings in the near future possible as an RCM is available to the institute. Additionally, use of the PolyMech mechanism and in some cases also the GRI mechanism led to failed simulations at around the ignition tempera-

tures when using the diesel engine parameters, making a study of the enhancing effects more difficult. All additive studies are based on a 2/1/1.5 mixture of COG, BFG, and air. It is common in the literature to give the amount of ignition enhancers that play a role in the ignition mechanism as a percentage of fuel [45, 46]. This procedure was followed in this work for the three ignition enhancers. As the amount of methane is directly correlated with other species from its primary mixture (COG), the amount of additive was calculated so that the proportions of all other species remained constant after the enhancer was added.

In addition to these chemicals, the effect of argon enrichment was investigated. Due to its low heat capacity, it allows the mixture to attain higher temperatures more easily. Due to the way the concentrations of ignition enhancers are listed, 1 % ozone indicates that the mole fraction of ozone is 1 % of that of methane, while 1 % argon denotes that a hundredth of the gas mixture consists of argon (in addition to any argon that is contained in air if included).

The effects of different additives on the ignition temperature are collectively depicted in Fig. 3.21 and explained below. The black line in Fig. 3.21 represents a mixture with a composition of 2/1/1.5 (COG/BFG/air) without any additives and serves as the baseline. As the  $y$ -axis denotes the ignition temperature (as defined above, the lowest initial temperature at which ignition occurs), the lower the line, the more reactive the mixture.

#### DME

Dimethyl ether (DME) has previously been shown to aid ignition for methane/oxygen mixtures [45, 47]. It has also been used in the RCM setup, replacing 10 % of methane to enhance ignition [9]. However, for this mixture simulations only predict significant improvements to the ignition temperature at high concentrations (10 %, grey line, square symbols in Fig. 3.21) and low engine speeds. Lower concentrations (1 %, cyan line, right-facing triangles) do not have an appreciable effect. In addition, the use of DME lowers carbon dioxide conversion if present in higher quantities. Therefore, DME does not project as a good ignition enhancer in the evaluated conditions.

#### Hydrogen peroxide

Hydrogen peroxide readily dissociates thermally, forms radicals quite easily and has been shown to decrease ignition delay in methane/air flames in simulations [46]. A reduced ignition delay would be beneficial to ignition temperature as the effects of ignition delay shown previously (see Section 3.2.4 on page 19) demonstrate. It is therefore a viable candidate for enhancing ignition in this mixture in order to lower the necessary temperature. As shown in Fig. 3.21, one percent of hydrogen peroxide (red line, circles) has a major effect on the ignition temperature, resulting in a decrease of up to 40 K compared to a mixture without any additives. The practicability of hydrogen peroxide for this

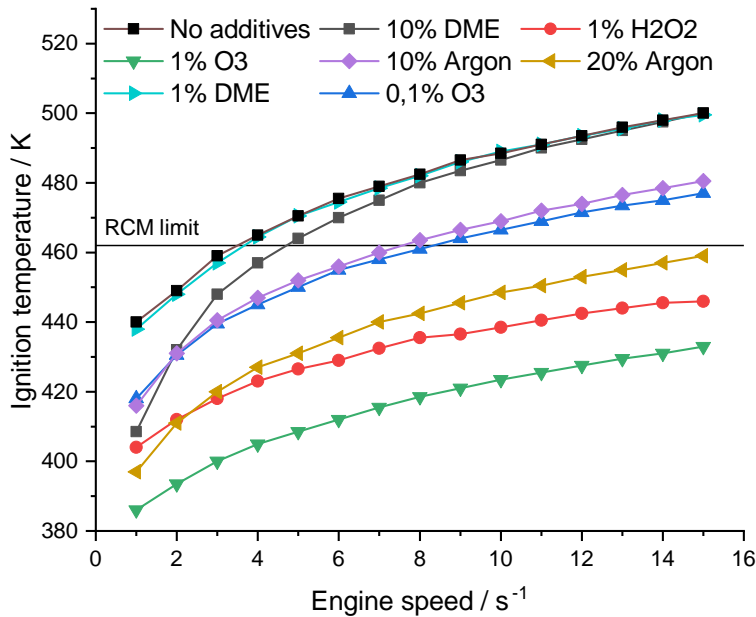


**Figure 3.21:** Effect of various additives on ignition temperature as functions of engine speed. The lower the values lie on the  $y$ -axis, the more reactive the mixtures is. The case without additives is represented by the black line with square symbols. The maximum initial temperature for the RCM lies at 462 K and is represented by a thinner black line.

use is questionable however, as it will likely undergo thermal decomposition before the initial temperatures targeted in this study and cause combustion during preheating.

### Ozone

Like hydrogen peroxide, ozone forms radicals quite readily, but is more thermally stable, and thus presents less of a risk of premature combustion. It has also been shown in experiments to increase the readiness for ignition in methane/air mixtures [48]. To study ozone as an ignition enhancer, the PolyMech mechanism was extended by a further 25 reactions with parameters from Starik et al. [32] and Howard and Finlayson-Pitts [33]. The simulations show that ozone projects as a powerful ignition enhancer and the most effective of those tested in this work, with a concentration of 1% (of methane, corresponding to 0.1% of the entire mixture) effecting an ignition temperature of 428 K at an engine speed of  $10 \text{ s}^{-1}/600 \text{ rpm}$  (green line, downward-facing triangles in Fig. 3.21). This value is 10 K lower than that of a mixture with addition of the same amount of hydrogen peroxide and more than 50 K lower than for a mixture without any additives.

Even an addition of 0.1 % (equivalent to a mole fraction of about 0.0001) ozone leads to a significant reduction in ignition temperature, almost allowing for ignition at the conditions the rapid compression machine is limited to, specifically its maximum initial temperature of 462 K. As the compression ratio of the machine is slightly adjustable, inducing ignition should be possible with this small amount of ozone added. At higher concentrations, ozone enables the conversion of  $\text{CO}_2$  at temperatures that require little heating of the primary gases. The effect of ozone concentration on ignition temperature is further detailed in Fig. 3.22.

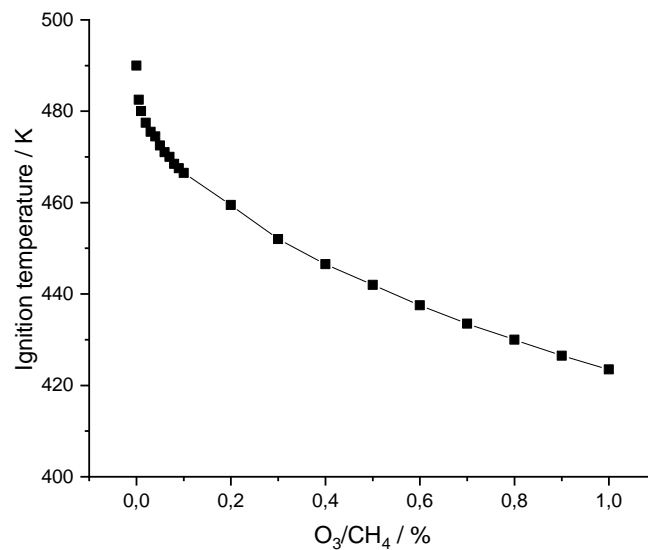


**Figure 3.22:** Effect of ozone/methane ratio (in %) on ignition temperature for RCM parameters (see Table 2.2 on page 8) and when applied to a composition of 2/1/1.5 (COG/BFG/air).

As the figure conveys, small concentrations of ozone already lower the ignition temperature drastically. At higher concentrations the effect dampens, but is still significant. Keeping in mind that a value of 1 % in the figure corresponds to a mole fraction of about 0.1 %, it becomes clear that minor, relatively easily generated amounts of ozone can significantly improve the reforming process.

The behavior of  $\text{CO}_2$  conversion as a function of the ozone/methane ratio is detailed in Fig. 3.23. It demonstrates that the conversion as a function of ozone concentrations follows similar behavior as other parameters, e.g. the temperature or the compression ratio, as the plot assumes a similar form. Before positive conversions are reached, more carbon dioxide is produced than consumed. The reason for this is again ignition delay. An increase in ozone concentration leads to a shorter ignition delay, which allows the dry reforming reaction to consume  $\text{CO}_2$  for a longer period of time, leading to

higher conversions. As with mixtures containing no additives, those containing BOFG ignite more easily, but achieve significantly lower conversions as the conditions (here the additive concentration) improve. Since the addition of ozone primarily allows ignition to occur at lower temperatures and does not impact the actual reforming reaction, the conversions are quite low (32% at 450 K and 1%  $O_3/CH_4$ ) due to the lower temperatures during compression. Compared to mixtures without any additives however, the addition of ozone greatly increases the  $CO_2$  conversion at any temperature.

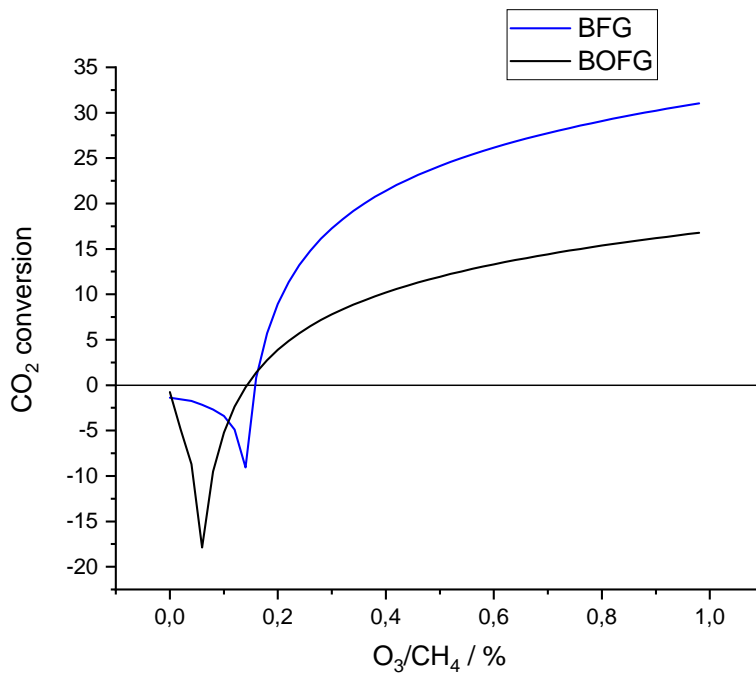


**Figure 3.23:** Effect of ozone/methane percentage on  $CO_2$  conversion in the reforming process for a gas composition 2/1/1.5 (COG/X/air, with X representing BFG (blue) or BOFG (black)).

### Argon

In a previous study under RCM conditions [9] argon was used to reduce the heat capacity of the overall mixture, thereby increasing temperature during compression. Due to the nature of this enhancement, the impact of the concentration is much more straightforward than for the additives which impact the combustion mechanism directly. The effect of the argon concentration is laid out in Fig. 3.24, showing a clear linear correlation between argon mole fraction and ignition temperature. Because of this, argon addition only impacts the mixture behavior significantly at much higher concentrations than ozone for example. Because of this, the reduced reforming capacity of the engine

must be considered. However, it enables reforming at lower initial temperatures, and is therefore a viable option for temperature-limited devices, for example the RCM.

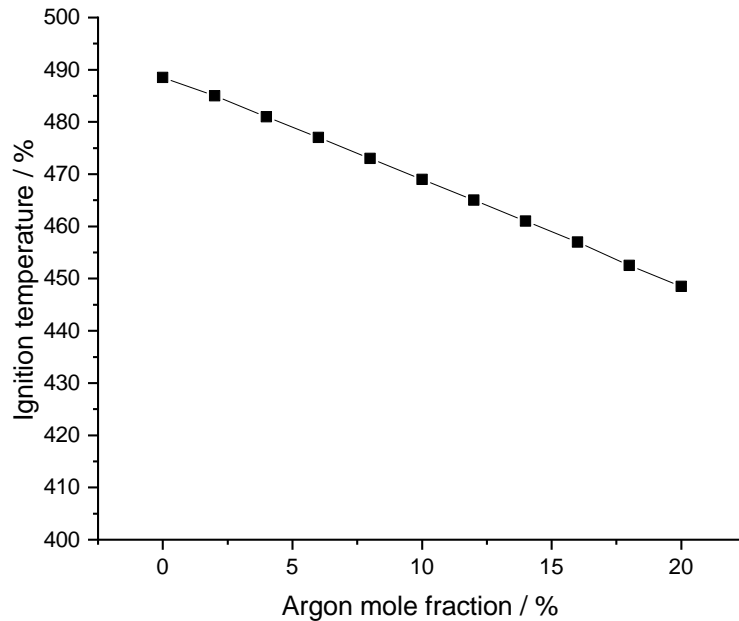


**Figure 3.24:** Effect of argon mole fraction on the ignition temperature of an 2/1/1.5 (COG/BFG/air) mixture at RCM conditions listed in Table 2.2.

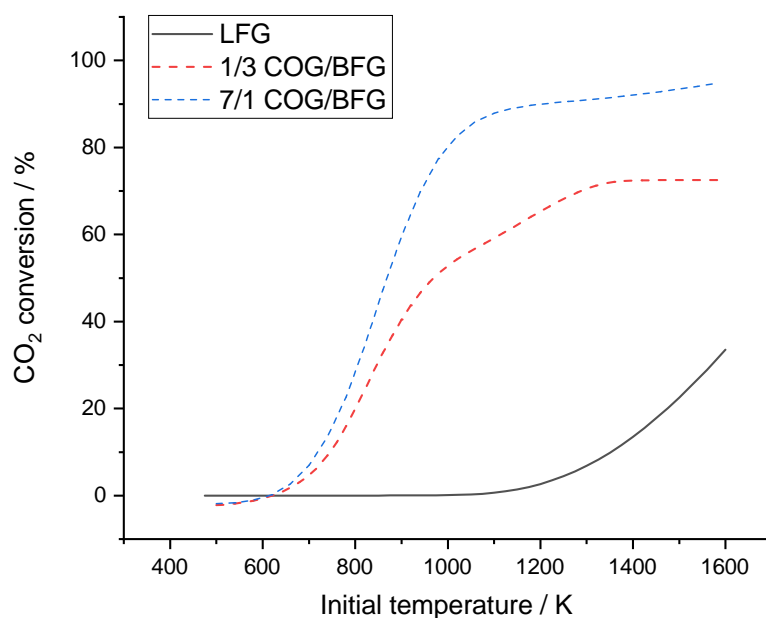
## 3.6 Landfill gas conversion in an internal combustion engine

In addition to steelworks off-gases, the conversion of carbon dioxide contained in landfill gas (LFG) has been investigated. The idea of reforming landfill gas is very attractive as it already contains significant amounts of both methane and carbon dioxide, while the concentrations of other species are low. Its exact composition varies depending on the wastes accepted by the facility and the amount of time between creation of the landfill and extraction of the gas [44]. An exemplary composition of landfill gas is listed in Table 3.4 along with the composition used for the simulations.

**Table 3.4:** Exemplary composition of landfill gas and mole fractions used for the modeling study.

	CH <sub>4</sub>	CO <sub>2</sub>	N <sub>2</sub>	other hydrocarbons
Percentage (actual) [44]	50-55	45-50	2-5	< 1
Percentage (simulation value)	50	45	4	1 (C <sub>2</sub> H <sub>6</sub> )

The possibility of reforming pure landfill gas in an internal combustion engine was investigated by varying the inlet temperature, with the results being presented in Fig. 3.25. The PolyMech model was also used for these simulations, as the conditions resemble the ones it was created and optimized for.

**Figure 3.25:** Comparison of CO<sub>2</sub> conversion for the dry reforming of landfill gas (black, solid) and air-free mixtures of COG and BFG (red and blue, dashed) as a function of the initial temperature.

While in theory the composition of landfill gas suits the prospect of dry reforming very well, as an almost stoichiometric ratio of methane and carbon dioxide is present, the process is predicted to require very high inlet temperatures. As dry reforming is strongly endothermic, it requires high temperatures to proceed in the desired direction. Because landfill gas does not contain any H<sub>2</sub>, the reverse water-gas shift reaction (Eq. 3.1) can not take place, and as shown in Section 3.1 (page 13), the actual dry reforming only sets in at much higher temperatures. As a comparison, two airless mixtures of COG

and BFG, where the reverse water-gas shift reaction is prevalent at lower temperatures, achieve considerable conversions at temperatures of above 800 K, as seen in Fig. 3.25. By contrast, the carbon dioxide in LFG is only significantly reformed above 1400 K.

To reduce the needed inlet temperatures, the landfill gas is mixed with air to enable combustion, thus providing the temperatures necessary for dry reforming. The mixture was optimized using the process described in Section 3.5.2 (page 34), the result of this optimization is depicted in Fig. 3.26.

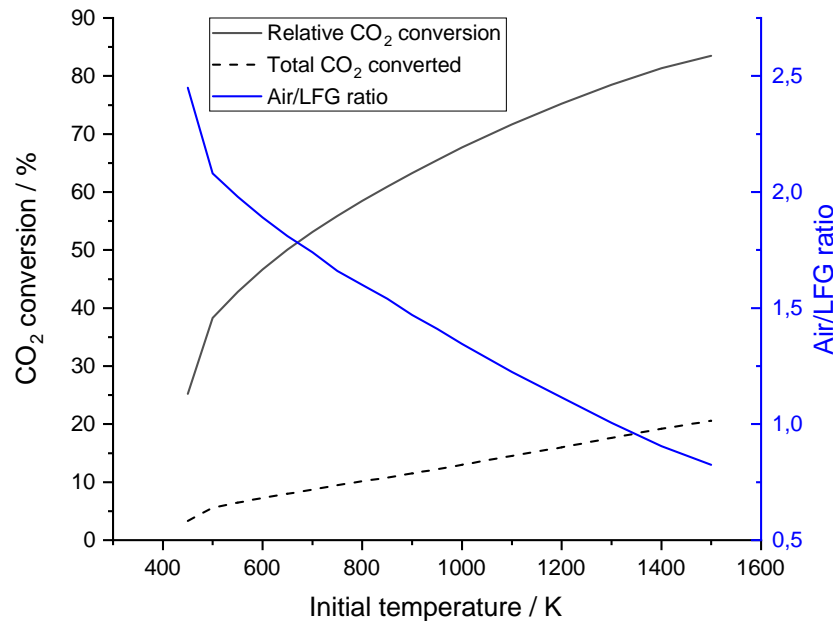


**Figure 3.26:** Maximum CO<sub>2</sub> conversion (black, solid, left axis) and total converted CO<sub>2</sub> (black, dashed, left axis) along with the optimal composition (blue, right axis) as functions of temperature.

The simulations predict that, akin to the previously examined COG/BFG/air mixtures, higher initial temperatures allow for richer LFG/air mixtures. The conversion also increases significantly with initial temperatures and combined with the richer mixtures cause the amount of converted carbon dioxide to increase consistently with the intake temperature. The total converted CO<sub>2</sub> eclipses 10% of the initial gas at 800 K, while the same value is only reached at 1200 K for a COG/BFG mixture and is never attained in the investigated COG/BFG/air mixtures. Due to the non-availability of the reverse water-gas shift reaction, the inclusion of air presents a marked improvement to the conversion of CO<sub>2</sub> contained in landfill gas. It reduces the temperature necessary for significant conversions (>20%) by about 700 K, resulting in a major drop in energy demands.

## 4 Conclusion and outlook

A wide-ranging modeling study concerning the dry reforming of carbon dioxide contained in industrial off-gases utilizing an internal combustion engine has been performed. The effects of a multitude of factors on the conversion of carbon dioxide from steelworks off-gases, which are a significant contributor to anthropogenic greenhouse gas emissions and in turn climate change, in an internal combustion engine have been evaluated. These factors include the geometric properties and operation parameters of the internal combustion engine and the initial state of the gas, comprised of its temperature, pressure and composition. Specifically, the composition was optimized with respect to the proportions of primary steelworks gases it consists of. Furthermore, studies were performed to evaluate the effect of various additives and the performance of mixtures without the presence of air. Additionally, dry reforming of landfill gas was investigated in regards to the conversion of the contained  $\text{CO}_2$ .

The numerical simulations were performed using the DETCHEM<sup>ENGINE</sup> program to model the internal combustion engine as a batch reactor with a variable volume profile. The model employed two chemical models, the GRI and the PolyMech mechanisms, and modeled heat transfer according to Woschni. The software tool CaRMeN was used to organize and automate simulations and enable the semi-automatic optimization process.

The model predicts substantial conversions of carbon dioxide from steelworks off-gases in the range of 40 % to 50 % at atmospheric initial pressures and initial temperatures of around 400 K. These conditions should be suitable for commercial internal combustion engines. Initial temperatures of more than 850 K enable conversions above 80 %. The studied process generates a product gas that primarily consists of nitrogen, hydrogen, carbon monoxide and water with smaller amounts of methane, carbon dioxide, and argon, depending on the exact initial composition and parameters used. The ratio of hydrogen to carbon monoxide in this product is dependent on the process parameters, but primarily lies in the range of 1.5-2, which makes it viable for chemical utilization, for example in Fischer-Tropsch processes or methanol synthesis. The simulations predict that the compression ratio, the engine speed and the inlet gas temperature have major impacts on the conversion of carbon dioxide. An optimization process provided the ideal composition of the inlet gas for a range of initial temperatures. Higher temperatures allow for richer mixtures, enabling higher  $\text{CO}_2$  conversions and absolute amounts of carbon dioxide converted. While the gas composition was optimized with respect to the relative conversion of carbon dioxide, a focus on the absolute amount of  $\text{CO}_2$  converted might also be advisable, as it is the economically more important quantity. Additionally, the reforming of basic oxygen furnace gas has been shown to not be as efficient as that

of blast furnace gas, as the former contains too much inhibiting carbon monoxide. It has also been determined that reforming can proceed without a prior combustion step, higher temperatures are necessary for this mode of operation however. The model also predicts that argon, hydrogen peroxide and especially ozone can increase the ignitability of the mixture and enhance the reforming process, allowing it to succeed with lower initial temperatures. In addition to steelworks off-gases, the reforming of landfill gas has been studied and shown to produce similar conversion levels.

As the results provided by the modelling study are promising, validation of the data in experiments would be a natural progression of this work. A rapid compression machine used in a previous study [9], for example, could be employed to test some of the results concerning additives affecting ignition temperature. Further studies could assess the energetic efficiency of this process, as has been carried out by Hegner and Atakan [49] for a similar polygeneration system, and examine its economic viability for industrial purposes. Another aspect of this process worth investigating further is the mode of ignition of the mixture. As the simulation utilizes a single-zone model, ignition is entirely caused by the compression of the combustible mixture. Alternative methods like spark ignition could potentially allow the initial temperature of the inlet gas to be reduced and therefore lower energy demands drastically and should be investigated further. Another fruitful area for further work might be the synthesis of more valuable products such as acetylene or formaldehyde in an engine by controlling engine speed, allowing the reaction mixture to be “frozen” at a desired composition. For example, acetylene has been predicted to appear in amounts of around 3 mol% during the dry reforming period for a typical mixture of steelworks off-gases by this model and it has been found that specific sets of parameters enable its preservation until the end of expansion.

# Bibliography

- [1] Climate Change 2014: Mitigation of Climate Change: Working Group III Contribution to the Fifth Assessment Report of the Intergovernmental Panel on Climate Change, OCLC: ocn892580682, Cambridge University Press, New York, NY, **2014**.
- [2] I. P. on Climate Change, Climate Change 2007: Synthesis Report Summary for Policymakers, IPCC, **2007**.
- [3] SETIS, Energy Efficiency and CO<sub>2</sub> Reduction in the Iron & Steel Industry, SETIS, **2011**.
- [4] T. J. Brown, N. E. Idoine, E. R. Raycraft, R. A. Shaw, S. F. Hobbs, P. Everett, E. A. Deady, T. Bide, World Mineral Production 2012-2016, British Geological Survey, **2018**, p. 96.
- [5] W. Uribe-Soto, J.-F. Portha, J.-M. Commenge, L. Falk, *Renewable and Sustainable Energy Reviews* **2017**, *74*, 809–823.
- [6] A. Hasanbeigi, L. Price, A. McKane, *The State-of-the-Art Clean Technologies (SOACT) for Steelmaking Handbook (2nd Edition)*, **2010**.
- [7] K. Takanabe, K. Nagaoka, K. Nariai, K.-i. Aika, *Journal of Catalysis* **2005**, *232*, 268–275.
- [8] L. A. Schulz, L. C. S. Kahle, K. H. Delgado, S. A. Schunk, A. Jentys, O. Deutschmann, J. A. Lercher, *Applied Catalysis A: General*, Nanocatalysis Science: Preparation, Characterization and Reactivity, dedicated to the scientific work of Jacques C. Vedrine. **2015**, *504*, 599–607.
- [9] H. Gossler, S. Drost, S. Porras, R. Schießl, U. Maas, O. Deutschmann, *Combustion and Flame (submitted)* **2019**, 10.
- [10] H. Goßler, *Partial Oxidation of Natural Gas in a Piston Engine: Modeling and Simulation*, **2014**.
- [11] O. Deutschmann, S. Tischer, C. Correa, D. Chatterjee, S. Kleditzsch, V. M. Jannardhanan, N. Mladenov, H. D. Minh, H. Karadeniz, M. Hettel, H. Gossler, **2018**.
- [12] J. Heywood, *Internal Combustion Engine Fundamentals*, 1st ed., McGraw-Hill Education Ltd, New York, **1989**.
- [13] G. Woschni in, National Fuels and Lubricants, Powerplants, Transportation Meetings, **1967**.

- [14] S. B. Fiveland, R. Agama, M. Christensen, B. Johansson, J. Hiltner, F. Maus, D. N. Assanis in, **2001**.
- [15] C.-J. Sung, H. J. Curran, *Progress in Energy and Combustion Science* **2014**, *44*, 1–18.
- [16] M. Werler, L. R. Cancino, R. Schiessl, U. Maas, C. Schulz, M. Fikri, *Proceedings of the Combustion Institute* **2015**, *35*, 259–266.
- [17] Hai Wang, Xiaoqing You, Ameya V. Joshi, Scott G. Davis, Alexander Laskin, Fokion Egolfopoulos, Chung K. Law, **2007**.
- [18] H. J. Curran, S. L. Fischer, F. L. Dryer, *International Journal of Chemical Kinetics* **2000**, *32*, 741–759.
- [19] C. K. Westbrook, M. Mehl, W. J. Pitz, G. Kukkadapu, S. Wagnon, K. Zhang, *Physical Chemistry Chemical Physics* **2018**, *20*, 10588–10606.
- [20] B. Chan, J. M. Simmie, *Physical Chemistry Chemical Physics* **2018**, *20*, 10732–10740.
- [21] D. L. Baulch, C. T. Bowman, C. J. Cobos, R. A. Cox, T. Just, J. A. Kerr, M. J. Pilling, D. Stocker, J. Troe, W. Tsang, R. W. Walker, J. Warnatz, *Journal of Physical and Chemical Reference Data* **2005**, *34*, 757–1397.
- [22] B. S. Haynes, H. G. Wagner, *Progress in Energy and Combustion Science* **1981**, *7*, 229–273.
- [23] Y. Hidaka, K. Sato, Y. Henmi, H. Tanaka, K. Inami, *Combustion and Flame* **1999**, *118*, 340–358.
- [24] C. Heghes, PhD thesis, University of Heidelberg, Germany, **2006**.
- [25] Z. Zhao, M. Chaos, A. Kazakov, F. L. Dryer, *International Journal of Chemical Kinetics* **2008**, *40*, 1–18.
- [26] G. Smith, D. Golden, M. Frenklach, N. W. Moriarty, B. Eiteneer, M. Goldenberg, C. T. Bowman, R. K. Hanson, S. Song, W. C. Gardiner, Jr, V. V. Lissianski, Z. Qin, GRI 3.0, <http://combustion.berkeley.edu/gri-mech/version30/text30.html>.
- [27] S. Porras, R. Schiebl, U. Maas in 8th European Combustion Meeting 2017, **2017**.
- [28] K. Hoyermann, F. Mauß, T. Zeuch, *Physical Chemistry Chemical Physics* **2004**, *6*, 3824–3835.
- [29] Y. Hidaka, H. Masaoka, H. Oshita, T. Nakamura, K. Tanaka, H. Kawano, *International Journal of Chemical Kinetics* **1992**, *24*, 871–885.
- [30] Y. Hidaka, T. Nakamura, A. Miyauchi, T. Shiraishi, H. Kawano, *International Journal of Chemical Kinetics* **1989**, *21*, 643–666.
- [31] Kaczmarek, Porras, Sen, Kasper, Schiebl, Maas, Atakan in 28. Deutscher Flammentag, Darmstadt, Germany, **2017**.

- 
- [32] A. M. Starik, V. E. Kozlov, N. S. Titova, *Combustion and Flame* **2010**, *157*, 313–327.
- [33] C. J. Howard, B. J. Finlayson-Pitts, *The Journal of Chemical Physics* **1980**, *72*, 3842–3843.
- [34] H. Gossler, L. Maier, S. Angeli, S. Tischer, O. Deutschmann, *Catalysts* **2019**, *9*, 227.
- [35] H. Gossler, L. Maier, S. Angeli, S. Tischer, O. Deutschmann, *Physical Chemistry Chemical Physics* **2018**, *20*, 10857–10876.
- [36] D. C. Siegl, R. M. Siewert, *SAE Transactions* **1978**, *87*, 2726–2736.
- [37] W. G. Berlinger, US6314924B1, **2001**.
- [38] E. Porpatham, A. Ramesh, B. Nagalingam, *International Journal of Hydrogen Energy* **2007**, *32*, 2057–2065.
- [39] S. D. Hires, R. J. Tabaczynski, J. M. Novak, *SAE Transactions* **1978**, *87*, 1053–1067.
- [40] H. Omidvarborna, A. Kumar, D.-S. Kim, *Renewable and Sustainable Energy Reviews* **2015**, *48*, 635–647.
- [41] G. Borman, K. Nishiwaki, *Progress in Energy and Combustion Science* **1987**, *13*, 1–46.
- [42] J. Chang, O. Güralp, Z. Filipi, D. N. Assanis, T.-W. Kuo, P. Najt, R. Rask in, **2004**.
- [43] K. Taube, *Stahlerzeugung kompakt: Grundlagen der Eisen- und Stahlmetallurgie / Karl Taube*, **1998**.
- [44] O. US EPA, Landfill Gas Energy Project Development Handbook, en, Overviews and Factsheets, **2016**.
- [45] B. Zhang, H. D. Ng, *Fuel* **2015**, *157*, 56–63.
- [46] V. I. Golovitchev, M. L. Pilia, C. Bruno, *Journal of Propulsion and Power* **1996**, *12*, 699–707.
- [47] Z. Chen, X. Qin, Y. Ju, Z. Zhao, M. Chaos, F. L. Dryer, *Proceedings of the Combustion Institute* **2007**, *31*, 1215–1222.
- [48] T. Nomaguchi, S. Koda, *Symposium (International) on Combustion* **1989**, *22*, 1677–1682.
- [49] R. Hegner, B. Atakan, *International Journal of Hydrogen Energy* **2017**, *42*, 1287–1297.